

Peptide-DNA conjugates as building blocks for de novo design of hybrid nanostructures

Danielsen, Mathias Bogetoft; Mao, Hanbin; Lou, Chenguang

Published in:
Cell Reports Physical Science

DOI:
[10.1016/j.xcrp.2023.101620](https://doi.org/10.1016/j.xcrp.2023.101620)

Publication date:
2023

Document version:
Final published version

Document license:
CC BY-NC-ND

Citation for pulished version (APA):
Danielsen, M. B., Mao, H., & Lou, C. (2023). Peptide-DNA conjugates as building blocks for de novo design of hybrid nanostructures. *Cell Reports Physical Science*, 4(10), Article 101620.
<https://doi.org/10.1016/j.xcrp.2023.101620>

Go to publication entry in University of Southern Denmark's Research Portal

Terms of use

This work is brought to you by the University of Southern Denmark.
Unless otherwise specified it has been shared according to the terms for self-archiving.
If no other license is stated, these terms apply:

- You may download this work for personal use only.
- You may not further distribute the material or use it for any profit-making activity or commercial gain
- You may freely distribute the URL identifying this open access version

If you believe that this document breaches copyright please contact us providing details and we will investigate your claim.
Please direct all enquiries to puresupport@bib.sdu.dk

Review

Peptide-DNA conjugates as building blocks for *de novo* design of hybrid nanostructuresMathias Bogetoft Danielsen,^{1,2} Hanbin Mao,³ and Chenguang Lou^{1,*}

SUMMARY

Inspired by nature, modern nanotechnology has enabled the bottom-up construction of molecular machines and nanorobots using two different biomolecular building blocks, DNAs or peptides. As an emerging research field, synergizing these two biomolecular codes into a single nanostructure has provided super-powerful molecular tools into the arsenal of modern nanotechnology. Among them, peptide-DNA conjugates possess both attributes of peptide and DNA and can be arbitrarily predefined in given structural configurations, standing out as unique nanoscale building blocks for *de novo* design of instrumental nanostructures that otherwise could not be composed by using DNA or peptides only. Herein, the term peptide is used in the broadest sense, including oligopeptide, polypeptide, and protein. In this tutorial review, we survey the main progress made within the past decade in how to use peptide-DNA conjugates as nanoscale bricks to self-assemble hybrid nanostructures for different chemical and biological purposes. A concise perspective is included for existing challenges and potential future research directions. Looking to the horizon, peptide-DNA conjugates may serve as key structural elements in the coming decade to enable the bottom-up construction of advanced molecular machines, even comparable to those cellular organelles evolved by nature.

INTRODUCTION

Directed self-assembly of building-block-like molecules is an alluring strategy to form large chemical structures, where the intermolecular interaction patterns between the building-block-like molecules are casted to nano-, micro-, and even up to macroscale levels to drive self-evolved assembling processes. Nature uses double-stranded (ds) DNA/RNA to encode the genetic information of most life forms on Earth via the Watson-Crick hydrogen bonds, namely cytosine paired with guanine (C-G) and thymine/uridine paired with adenine (T/U-A). These two highly specific base-pair interactions have been repurposed to cause a boom in the development of DNA nanotechnology within the past few decades. Since the concept was proposed by Seeman in the 1980s,^{1,2} a wide range of DNA nanoscale architectures have been assembled to customize different chemical, biological, diagnostic, and/or therapeutic purposes. The DNA nanotechnology leaped into a new era when Rothemund invented the DNA origami technology at the beginning of this century.³ This programmable molecular tool was further empowered by integrating other non-canonical interactions such as Hoogsteen hydrogen bonds, cation chelation, and blunt-end π - π stacking. However, the chemical compositions of DNA nanostructures alone are limited to the functional groups of four nucleotides, namely two purine nucleotides (A and G) and two pyrimidine nucleotides (C and T), which inherently makes them lack diverse chemical functions. Aptamers and DNazymes

¹Department of Physics, Chemistry and Pharmacy, University of Southern Denmark, Campusvej 55, 5230 Odense M, Denmark

²Department of Chemistry and Biochemistry, University of Colorado at Boulder, Boulder, CO 80309, USA

³Department of Chemistry and Biochemistry, Kent State University, Kent, OH 44242, USA

*Correspondence: chenguang@sdu.dk
<https://doi.org/10.1016/j.xcrp.2023.101620>



are two exceptional modalities, capable of binding to specific targets or catalyzing different types of chemical reactions over a wide range of substrates (DNA, RNA, porphyrin, thymidine dimer, nucleopeptides, amino acids, esters, amides, etc.); however, almost all of them are composed of single-stranded (ss) nucleic acid sequences and thus are not regarded as nucleic acid nanostructures.^{4–8} Antisense technologies are interfering pathways to regulate gene expression by using ss oligonucleotides (ONs) or ds RNAs with the help of auxiliary enzymes and protein complexes, which also fall out of nucleic acid nanostructures.^{9,10} The same principle also applies to triplex technology,¹¹ molecular beacons,¹² and mRNA vaccines¹³ where only ssDNA or ssRNA sequences are involved. Toehold-mediated strand displacement has been widely used for signal amplification of various biological cues, but the systems are composed of separate ss ONs.¹⁴ Readers are referred to other comprehensive reviews for these applications.^{4–18}

When the genetic information is decoded from DNA/RNA, nature uses 20 canonical amino acids to compose other types of biopolymer protein that are responsible for most cellular biological functions. After they are translated in the ribosome, the proteins are transported to the endoplasmic reticulum for correct folding. The primary protein structures fold to form the secondary structures (such as α helices and β sheets) and then to their tertiary and quaternary structures (such as coiled coils and subunit associations) to acquire skeletal mechanics, tensile elastics, catalytic activities, and/or recognition abilities. In the last two decades, highly specific interaction patterns of the secondary/tertiary structures in natural proteins have been leveraged to the surge of peptide nanotechnology for the *de novo* design of enzyme mimics and the bottom-up construction of artificial protein structures.¹⁹ For a thorough overview, we suggest exploring other recently published reviews.^{20–23} Despite significant progress that has been made in structural peptide/protein nanotechnology, the intricate sequence-structure relations are not fully understood yet. How to maneuver the protein functions like nature by actuating several amino acid residues and/or short peptide motifs of their primary sequences is not fully known. Given the versatile biological functions offered by 20 amino acid building blocks, the structural peptide/protein nanotechnology is limited by the lack of programmability from one-dimensional (1D) primary sequence to three-dimensional (3D) topological folding.

A rational design principle is to coherently combine these two powerful nanoworld codes, DNA and proteins/peptides, into a single macromolecule to synergize the high structural programmability of DNA nanotechnology and versatile chemical functions offered by peptides/protein sequences. This strategy is surmised to unveil a new chemical dimension that the single use of each modality is unable to access. Gratifyingly, although the research field is only slowly emerging in recent years, significant progress has been made to illuminate the power of this unique molecular tool for various chemical and nanotechnological applications. In this tutorial review, we introduce the seminal works and milestone advances made within the past decade to provide a retrospective for this new research area. We set the following criteria to highlight the vital role of cross-domain synergy between DNA and peptides/proteins in the hybrid nanostructures: (1) DNA component strands and peptides/proteins are covalently conjugated, (2) both the DNA domain and the peptide/protein domain can be self-assembled in an orthogonal manner, (3) each domain has more than one component strand, (4) the self-assembly processes are highly cooperative via intermolecular interactions, and (5) cross-domain interactions are allowed for higher-order structures. A few non-covalent conjugation examples are also included to demonstrate a broad sense of DNA-peptide/protein

conjugates for nanotechnological uses. However, due to the space limit, we apologize that we are unable to cover all the progress made in this emerging research field. For an in-depth overview of DNA-peptide/protein conjugates for other applications such as surface display, templated functional assembly, enzyme cascades, protein/peptide encapsulation, and targeted delivery, we refer the readers to other excellent reviews/articles published recently.^{11,24–28}

In the following sections, we briefly introduce the commonly used chemical methods for bioconjugation of DNA to peptides/proteins. Afterward, four different subsections are included in order of increasing hierarchical complexity to demonstrate that peptide-DNA conjugates can be exploited as building-block-like parts to assemble various hybrid nanostructures: (1) using peptide-ON conjugates to assemble hybrid nanostructures, (2) using peptide-DNA nanostructure conjugates to assemble hybrid nanostructures, (3) using protein-ON conjugates to assemble hybrid nanostructures, and (4) using protein-DNA nanostructure conjugates to assemble hybrid nanostructures. Finally, concise conclusions are given for the current challenges and our perspectives.

CHEMICAL METHODS TO COMPOSE PEPTIDE-DNA CONJUGATES

Various chemical methods have been developed to connect peptides to DNAs either covalently or non-covalently, catering for different chemical and biological purposes. The covalent ligation produces a stable DNA-peptide hybrid macromolecule and, in most cases, is realized via aminoacylations, orthogonal reactions, Michael additions, and thiol oxidations (Figures 1A–1G). The non-covalent conjugation, however, takes advantage of the high binding affinity between two cognate entities (one attached to DNAs and the other fused to peptides) to confine the DNA and peptide modalities in proximity via protein-protein, protein-ligand, and ligand-ligand interactions (Figure 1H). Given the main topic as the recent progress of peptide-DNA conjugates in chemical and nanotechnological applications, in this section, we first elaborate on several user-friendly covalent methods that have been widely used for quantitative DNA-peptide ligations. In these cases, small linkages are formed between peptides and DNAs and thus are considered not to significantly perturb the DNA and peptide functions. Then we briefly introduce the non-covalent conjugation method. Other means that generate bulky linkers are out of the scope in this section, and we recommend that interested readers explore recent reviews on the topic.^{24,26,27}

Aminoacylation is widely used for DNA-peptide conjugation, where a new amide bond is formed between an amino function and an activated carboxylic acid group usually in the form of an NHS ester (Figure 1A). This method is highly efficient when all free amine groups need to be acylated; for example, Nardin et al. reported successful conjugations between amino-modified DNAs and dipeptides whose C-terminal carboxylic acids were activated.^{29–32} This method is also useful for attaching multiple DNAs to a single protein where the lysine residues on the protein surface can be readily reacted with the NHS-ester warhead. The DNA strands carrying the activated NHS esters can be obtained by first incorporating amino functions and then reacting them with homo-bifunctional linkers in excess (*vide infra*).³³ A drawback of the aminoacylation chemistry is the lack of regiospecificity; all exposed amine residues can be reacted with the activated esters. This can be problematic when the defined number of DNAs should be attached to proteins, or a single DNA strand needs to be conjugated to a specific amine residue of the protein. In

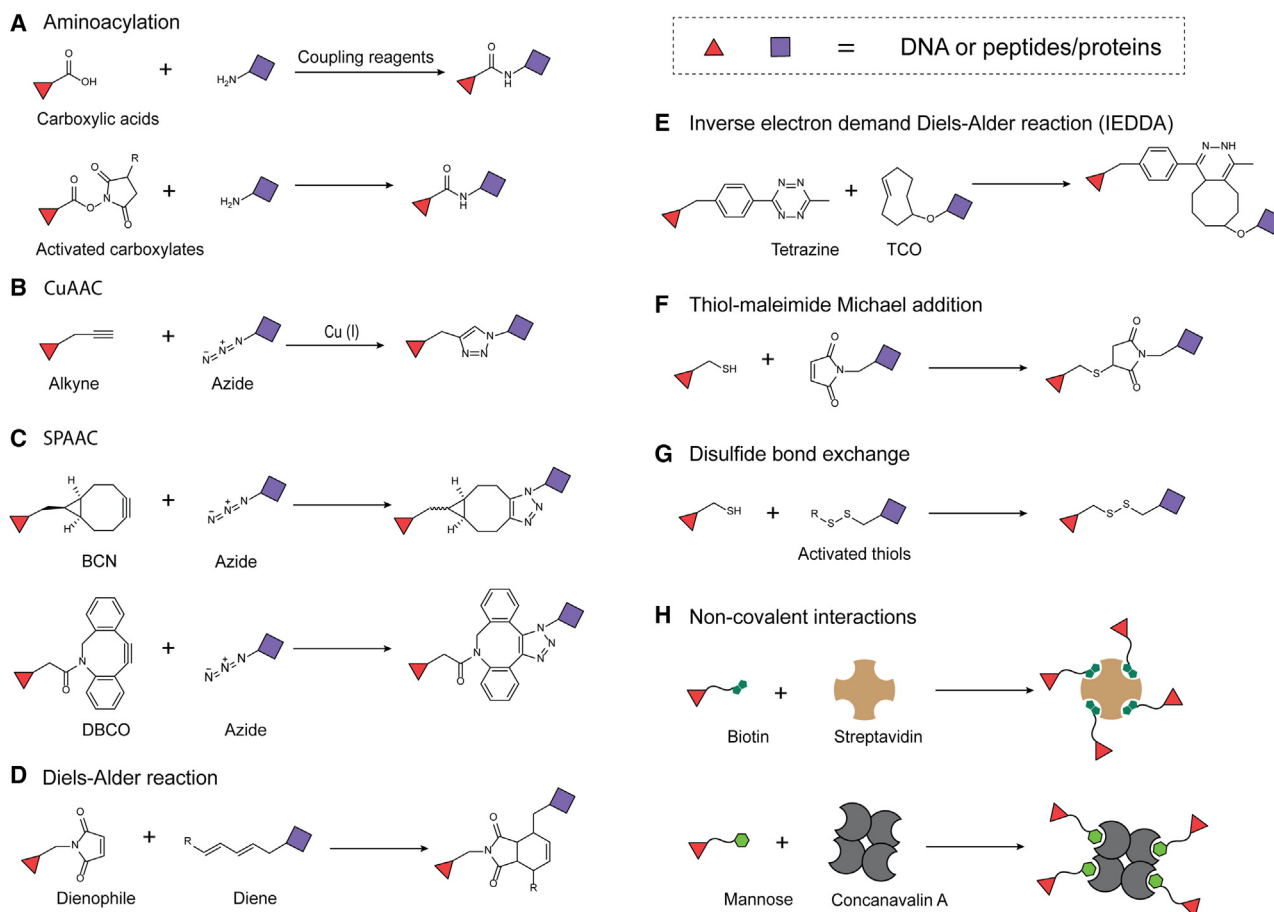


Figure 1. Commonly used methods for conjugation of DNA to peptides/proteins

Common methods include, but are not limited to, aminoacylation (A), CuAAC (B), SPAAC (C), Diels-Alder reaction (D), inverse electron demand Diels-Alder reaction (E), thiol-maleimide Michael addition (F), disulfide bond exchange (G) and non-covalent interactions (H).

addition to the aminoacylation, Schiff base formation has also been reported for peptide-DNA conjugation.³⁴

Orthogonal reactions have been widely used to ligate DNAs and proteins/peptides, among them copper-catalyzed alkyne-azide cycloaddition (CuAAC)^{35–42} and strain-promoted alkyne-azide cycloaddition (SPAAC)^{43–55} predominate in this area (Figures 1B and 1C). The reaction handles can be efficiently introduced into DNA, peptides, and proteins. Most short DNA sequences are obtained via solid-phase DNA synthesis, to which reaction handles can be furnished in a customized manner. Likewise, reaction handles can be specifically addressed at sub-nanometer resolution for DNA nanostructures/origamis by introducing the corresponding modified staple strands. In the case of peptides and small proteins accessible to solid-phase synthesis, reaction handles can be incorporated via artificial building blocks or modified amino acids almost in an arbitrary manner. For large proteins, genetic coding of non-canonical amino acids via bacteria expression systems is the most common way to introduce the reaction handles. The resulting peptides/proteins are then reacted with the DNAs to achieve the desirable peptide-DNA or protein-DNA ligations. Various peptides, proteins, and viral capsids have been conjugated to short DNA sequences and DNA origami structures via either CuAAC or SPAAC reactions in the below sections. In addition, other

highly specific reactions have also been employed to crosslink DNA and peptides/proteins, such as Diels-Alder reactions^{56,57} (Figure 1D) and inverse-electron-demand Diels-Alder reactions^{52,58} (Figure 1E).

Alternative methods to ligate DNAs and peptides include the Michael addition^{33,42,59–63} (Figure 1F) and the disulfide bond formation^{51,53,54} (Figure 1G). Herein, Michael addition refers to using the thiol groups as Michael donors and can be used to achieve site-specific ligation owing to the rare presence of cysteine residues in natural proteins. For those proteins that do not have cysteine residues or have them buried deep inside the proteins, point mutations can be introduced via protein engineering to display the wanted number of cysteine residues on the protein surface for DNA conjugation (the Michael acceptors are attached to DNAs, such as α,β -unsaturated carbonyl warheads). Parallel to the Michael addition, when a second thiol function is present in DNAs, the two thiol groups can be reacted with each other to form a disulfide bond between the protein/peptide and DNA in oxidative conditions. Please note that the resulting disulfide bond is not a stable linker that can be easily reduced to two separate thiols in the presence of reductants (glutathione [GSH], dithiothreitol [DTT], tris(2-carboxyethyl)phosphine [TCEP], etc.) and thus reverse the protein-DNA ligation.^{53,54}

Benefitting from the natural amino acid residues (lysine and cysteine) of peptide/proteins and the convenience to incorporate chemical functions (amino group, thiol, alkyne, dibenzocyclooctyne [DBCO], bicyclononyne [BCN], *trans*-cyclooctene [TCO], etc.) into ONs via phosphoramidite chemistry, two different reactions are usually combined to facilitate peptide-DNA bioconjugation (Figure 2). Bifunctional linkers are commercially available for turning the chemical functions of peptide/DNA to the wanted reaction handles, ready for the desirable crosslinking. Some strategies are also discussed in the below sections: (1) changing the pre-installed amino groups of DNA to strained alkynes, which are then conjugated to the azido functions of peptide/proteins via SPAAC or by swapping the two click handles the other way around^{45–54,64}; (2) turning the epsilon-amine of lysine residues or the free thiols of cysteine residues of peptide/proteins to azido functions that are clicked to alkyne-modified DNAs through CuAAC or inverting the two click handles^{37,41,42}; (3) converting the exotic amino groups of DNA to maleimide functions for crosslinking to the free thiols of peptide/proteins via Michael addition, where the two functional groups are exchangeable^{33,42,59–61,63}; (4) adapting the free amino groups of DNA to activated thiol functions for conjugation with the cysteine residues of peptide/proteins through thiol-disulfide exchange^{51,53,54}; and (5) transforming the lysine residues of peptides/proteins to tetrazine functions that can be clicked to TCO-modified DNA via inverse electron demand Diels-Alder reaction.⁵²

Finally, the connection of peptides to DNAs was also realized via non-covalent interactions (Figure 1H). One of the most popular methods (Figure 1H, top) takes advantage of the highly specific binding event between streptavidin and biotin.^{65,66} The dissociation constant (K_D) was reported to be as low as 10^{-14} M for monovalent binding,⁶⁷ and thus the binding strength is considered comparable to covalent crosslinking. In addition, mannan-concanavalin A (ConA) interaction was also utilized to produce stable DNA-peptide hybrid structures (Figure 1H, bottom),⁶⁸ but it was found to be weaker than the biotin-streptavidin interaction. Coordination chemistry was also developed for non-covalent DNA-peptide crosslinking using hexahistidine (His_6)-containing proteins and nitrilotriacetic acid-modified DNAs in the presence of a nickel cation as the coordination center.^{69–71} Other methods have also been reported for non-covalent peptide-DNA crosslinking, including

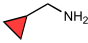
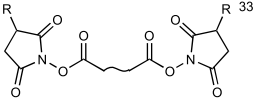

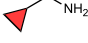
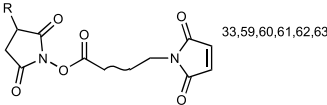
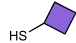
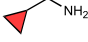
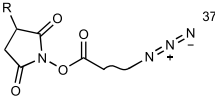

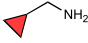
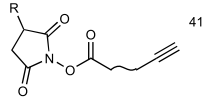
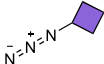
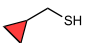
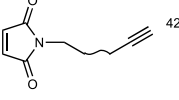
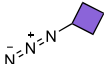
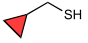
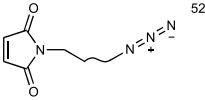
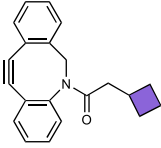
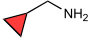
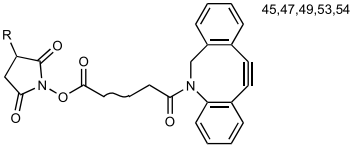
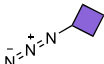
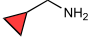
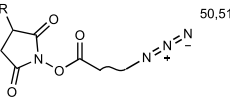
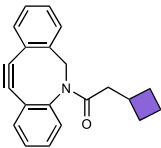
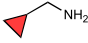
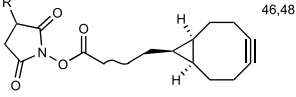
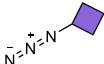
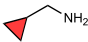
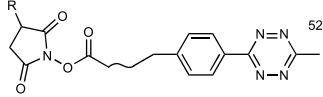
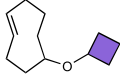
DNA/peptides	Reactions	Bifunctional linkers	Reactions	DNA/peptides
	Aminoacylation		Aminoacylation	
	Aminoacylation		Michael addition	
	Aminoacylation		CuAAC	
	Aminoacylation		CuAAC	
	Michael addition		CuAAC	
	Michael addition		SPAAC	
	Aminoacylation		SPAAC	
	Aminoacylation		SPAAC	
	Aminoacylation		SPAAC	
	Aminoacylation		IEDDA	

Figure 2. The homo-bifunctional and hetero-bifunctional linkers are widely used for DNA-peptides/proteins conjugation
The listed ones have been used in the select seminal works and milestone advances (*vide supra*).

electrostatic/specific peptide-DNA interactions,^{25,72} ligand-aptamer interactions,⁷³ natural protein-protein interactions,⁷⁴ and protein-DNA interactions.^{75–78}

USING PEPTIDE-DNA CONJUGATES TO ASSEMBLE HYBRID NANOSTRUCTURES

In this section, we start from the simplest peptide-ON conjugates (POCs) composed of oligopeptides and short-ON component strands. Then the structural complexity will be increased from ONs to DNA nanostructures and from oligopeptides to proteins. Finally, the hybrid protein-DNA nanostructures are exemplified.

OLIGOPEPTIDES/POLYPEPTIDES CONJUGATED TO ONs AS THE MONOMERIC UNITS

Extended secondary/tertiary structures in both DNA and peptide domains

The nanoconstructs described in this subsection consist of peptide and DNA domains that do not have finite secondary or tertiary structures before or after self-assembly. Such peptide-DNA systems usually consist of nonstructured peptide and/or DNA subdomains, from which diverse and complex hybrid architectures have been self-assembled.

Verbert-Nardin and co-workers reported a user-friendly synthesis method of covalently conjugating a 12-mer polypyrimidine sequence to a diphenylalanine (FF) dipeptide by joining the 5' end of the ON to the C termini of the dipeptide via amide bond formation (Figure 3A).³² When they were separated, the polyanionic nature of ON made it well solvated by water molecules and cation screening in aqueous conditions, whereas the hydrophobic FF domain was prone to self-assemble to form fibrillar structures.⁷⁹ Conjugating the hydrophilic ON to the hydrophobic FF domains induced a morphology change from linear fibrils (FF dipeptide alone) into hollow spherical structures. For the latter, a double layer of hydrophilic ONs was formed, one being exposed to the interior cavity and the other to the external aqueous environment. Meanwhile, the conjugated FF domains were tightly stacked against each other in the middle of the double layer to stabilize the whole spherical structure. In contrast, co-incubation of preformed FF fibrils and free ONs was found to disrupt the fibrils and fail to produce any spherical structures, showing that the covalent conjugation played a key role in the POC self-assembly. Interestingly, the spherical morphology was disrupted when urea was added (chaotropic agent). This implied that hydrogen bonds may be formed between the neighboring ON strands, which could contribute to stabilizing the spherical structures. The self-assembled structures were proposed to be used as responsive nanocarriers for drug delivery. When sulforhodamine B was encapsulated as a model compound, the spherical structures released the fluorophore molecules responsive to the pH decrease from 6.5 to 4.5. The destabilizing effect was ascribed to cytosine protonation in the hydrophilic ON domain, highlighting that both the ON and FF domains play indispensable roles in the spherical structure formation.

The concept was further developed by Goodwin and co-workers, who designed a potential delivery system using the FF dipeptide attached to either a DNA strand or polyethylene glycol (PEG5000) via a pH-responsive hydrazone bond (Figure 3B).³⁴ The N-terminal amino groups of the FF dipeptide were alkylated using 4-(bromomethyl)-benzaldehyde. The PEG5000 and poly-T strand (15-mer) were designed to have a hydrazide function. An intermolecular crosslinking between the aldehyde and hydrazine groups resulted in hydrazone formation. The authors then mixed the two hybrid molecules in different ratios to form the wanted vesicular

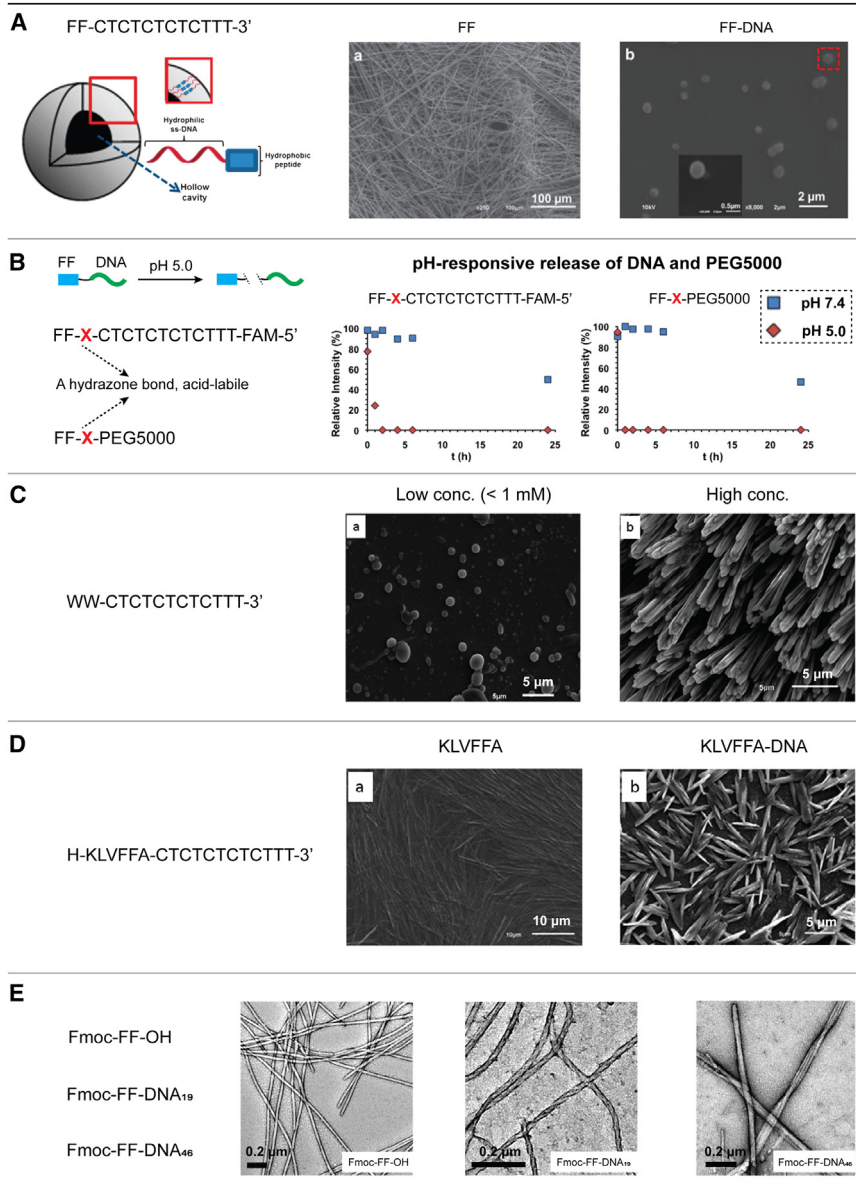


Figure 3. The peptide and DNA domains self-assembled into extended secondary/tertiary structures in the different nanoscale architectures

(A) Spherical structures formed by FF-DNA conjugates. Reproduced with permission from Gour et al.³² Copyright 2012, Royal Society of Chemistry.

(B) pH-responsive spherical structures formed by FF-PEG5000 and FF-DNA conjugates. Reproduced with permission from Hafenstine et al.³⁴ Copyright 2015, John Wiley and Sons.

(C) Macromolecular self-assemblies formed by WW-DNA conjugates. Reproduced with permission from Gour et al.³¹ is licenced under CC BY 3.0.

(D) Controlled aggregation of KLVFFA-DNAs. Adaptation from the article by Gour et al.,³⁰ Copyright 2015, Elsevier.

(E) Responsive supramolecular architectures composed of Fmoc-FF-DNAs and Fmoc-FF-OH. Adapted with permission from Daly et al.⁴⁷ Copyright 2019, American Chemical society.

structures. No significant change was observed between the formed vesicles, either when incubating the FF-PEG system alone or as a mixture between the FF-DNA/FF-PEG constructs. As expected, the hydrazone bond cleavage was triggered when the pH was lowered from pH 7.4 to pH 5, leading to the separation of the FF and DNA

domains. The released FF molecules then self-assembled to form fibrils without any DNA component trapped inside.

In a follow-up study, Vebert-Nardin et al. replaced the FF domain with a ditryptophan (WW) dipeptide to explore further the macromolecular self-assembly (Figure 3C).³¹ Thus, the WW dipeptide was conjugated to the 12-mer polypyrimidine DNA sequence via an amide formation. When the resulting WW-DNA hybrid molecule was incubated in the given experimental condition, two different macromolecular self-assemblies could be formed. With low concentrations of WW-DNA hybrid molecules, spherical nanostructures were produced. However, at the high concentration, fibrils were obtained. The spherical structures were facilitated by the π - π stacking between the WW domains and the hydrogen bonds between the DNA component strands. The latter interaction was found to be vital. The spherical structures were dissociated upon addition of either urea or complementary DNA strands. The inherent fluorescent property of the conjugated WW domain opened a door toward label-free optical sensing of nucleic acid strands for diagnostic applications.

To better understand the controlled aggregation of peptide-DNA hybrid molecules, Nardin and co-workers further replaced the WW dipeptide with a hexapeptide, KLVFFA (Figure 3D).³⁰ This 6-mer peptide sequence is derived from the central hydrophobic core of amyloid- β peptides and is indispensable for the pathological aggregation of amyloid- β peptides to form neurotoxic oligomers and fibrils associated with the onset of Alzheimer's disease.⁸⁰ This hexapeptide was covalently conjugated to the same 12-mer polypyrimidine DNA sequence in a similar manner. The resulting KLVFFA-DNA conjugate could self-assemble into amyloid-like fibers in the given experimental conditions. When the complementary DNA strand was present, the self-assembly process was reoriented to produce spherical structures. In the latter case, the induced morphology change was ascribed to the hydrogen bonds being significantly disrupted between the conjugated DNA strands. The preformed peptide-DNA fiber was not perturbed by adding the same DNA complement, showing that the hydrogen bonds were well shielded. Decreasing the pH from 7.2 to 2.5 resulted in the protonation of the N3-position of the cytosines, which in turn weakened the hydrogen bonds between the conjugated DNA strands and disrupted the planar nature of the fibrils, finally leading to the formation of spherical structures. Taken together, these results highlighted the contribution of the hydrogen bonds between the conjugated DNA strands to drive the aggregation of the hexapeptide-DNA hybrid molecules to form amyloid-like fibers.

The hydrophobic stacking of FF dipeptide to form fibers and the Watson-Crick base pairing of complementary DNA strands to form double helices were both utilized by Freeman and co-workers to construct responsive supramolecular architectures composed of peptide-DNA copolymers (Figure 3E).⁴⁷ The FF dipeptide retained a Fmoc group at the N terminus and was modified with an azide group at the C-terminal residue. A 19-mer DNA sequence was designed to have a DBCO function. The SPAAC reaction between the Fmoc-protected FF dipeptide and the DNA sequence resulted in the desired FF-DNA hybrid molecule. In the freshly prepared FF-DNA₁₉ solution, short filament structures were formed. In contrast, when the FF-DNA₁₉ solution was annealed, very long twisted fibers were formed. Adding a DNA intercalator dye and DNA complements to the preformed FF-DNA₁₉ fibers revealed that only around 5% of the total ssDNA component was available for hybridization; 95% of the conjugated ssDNA strands remained unhybridized and persisted on the surface of the FF-DNA₁₉ bundles. These findings inspired the authors to mix two complementary DNAs, each carrying a Fmoc-FF moiety. In addition to the expected fibers,

larger twisted bundles were also formed, probably due to the multiple cross-fiber hybridization events of complementary DNAs. The dimensions of these twisted bundles were further tuned by temperature change and strand displacement to demonstrate the reversibility of this assembled hierarchical structure. Meanwhile, the authors also elongated the DNA sequence from 19-mer to 46-mer to explore whether the DNA length could influence the self-aggregation process. Significant changes were noticed in the morphology, dimension, and helicity of the resulting long FF-DNA₄₆ fibrils. Overall, the studies in this section highlight that both peptide and DNA components of the peptide-DNA hybrid molecules contributed significantly to the self-assembly process. The resulting nanoscale architectures could be actuated by changing various parameters, including pH, concentration, temperature, time, complementary DNA, differences in peptide sequences, ionic strength of the buffer, and DNA length.

Finite canonical/non-canonical secondary structures are formed in the DNA domains

Most proteins must fold into their specific 3D configurations to impart target recognition and catalytic functions. For many of them, a decent proportion of the whole protein motif acts as a templating scaffold to organize the active site composed of amino acid residues and/or short peptide motifs. A rational design of artificial protein structures is to explore the possibility of using stable and programmable biomaterials to replace these vulnerable proteogenic scaffolds to engineer the amino acid and peptide display in a precise manner. For example, Hamilton et al. pioneered the use of a non-canonical nucleic acid secondary structure to confine two looped peptide strands in proximity to imitate the antibody-binding domain (Figure 4 A).³⁶ A pair of guanosine-rich ssDNA sequences were conjugated to the C and N termini of each peptide via the CuAAC reaction. Two different peptides were used in this study. The two ssDNAs could self-assemble into either a homogeneous or heterogeneous G-quadruplex in the presence of an alkali cation (K⁺ or Na⁺). Thus, the self-assembly of four ssDNAs induced two different peptide configurations, two peptide strands being anchored on the same face or on the two opposite faces of the G-quadruplex scaffold. A tetrameric form was also noticed, where four peptides were sandwiched by two G-quadruplex structures. The self-assembly of peptide homodimer and heterodimer on the same face of the G-quadruplex template was further explored. This study unveiled that DNA secondary structures could serve to template artificial protein mimics of antibody-binding domains.

Taking a step further, Lim and Kye coherently combined two different biomolecular interactions, peptide β sheet formation and DNA duplex hybridization, to realize the *de novo* design of deoxyribonucleoproteins (Figure 4B).³⁸ The peptide contained a 13-mer segment for β sheet self-assembly, which was sandwiched by an alkyne function at the N terminus and a trimeric arginyl-glycyl-aspartic acid (RGD) repeat at the C terminus. The alkyne function was used for DNA conjugation via the CuAAC reaction, and the extended RGD repeat was designed to promote cell internalization. Each ssDNA sequence was chemically modified with an azide function at the 5' end. The click ligation between the peptide and DNA was accomplished through an on-resin fragment ligation method, where the free peptide was conjugated to the ssDNAs that were anchored to the solid supports. The desired peptide-DNA conjugates were then cleaved from the supports. The peptide was clicked to two different ssDNA sequences; one was a 20-mer antisense strand that could bind to the sense mRNA to inhibit the green fluorescent protein (GFP) expression, and the other served as a passenger strand (18-mer). When the two peptide-ssDNA conjugates were mixed in an equimolar concentration, a toroid-shaped nanoassembly

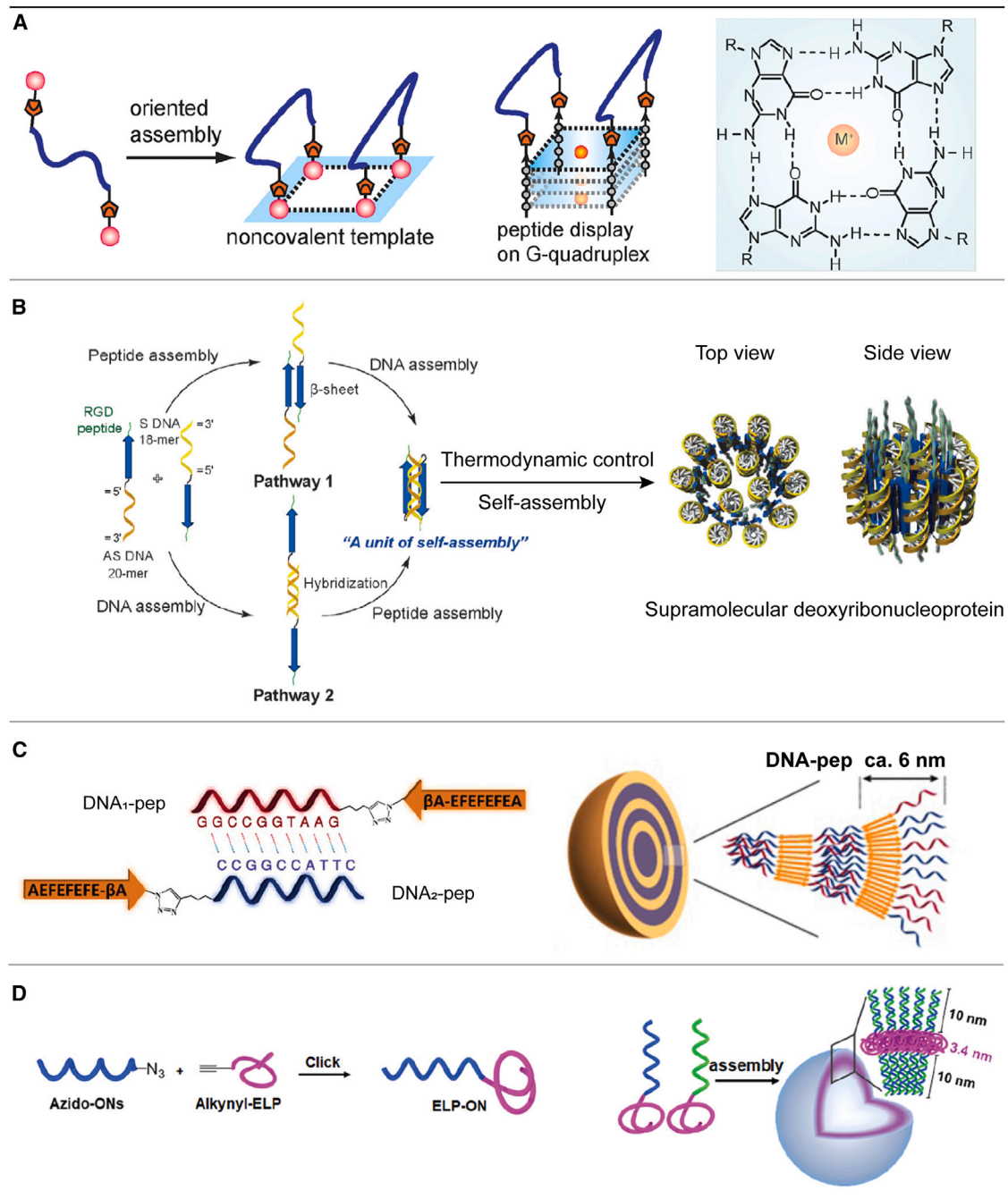


Figure 4. Peptide-DNA conjugates self-assembled into various nanoscale architectures where finite canonical/non-canonical secondary structures were formed for the DNA domains

(A) Two looped peptide strands were templated by a G-quadruplex formation. Adapted with permission from Ghosh et al.³⁶ Copyright 2012, American Chemical Society.

(B) *De novo* design of deoxyribonucleoproteins. Adapted with permission from Kye et al.³⁸ Copyright 2016, Wiley-VCH.

(C) Concentric bilayer nanostructures formed by (EF)_n-DNA conjugates. Adapted with permission from Chotera et al.³⁵ Copyright 2018, Wiley-VCH.

(D) Programmable self-assembly of temperature-responsive nanospheres. Reproduced with permission from Wang et al.³⁹ Copyright 2021, Royal Society of Chemistry.

was obtained, of which four dsDNA helices and one β sandwich were aligned perpendicularly to the 9-nm diameter circular plane. The dsDNA helices were located close to the toroidal surface, while the β sandwich was buried inside the toroidal tube. The hydrophilic RGD repeat also resided at the toroidal surface. The central pore formation was due to the electrostatic repulsion between the central dsDNA helices. When the peptide β sheet formation preceded the DNA duplex hybridization, homogeneous toroids were observed. The same architectures were obtained when the self-assembly order was reversed. Such structure formation enjoys the privileged synergy between the two different types of biomolecular interactions. This toroidal object was explored further as a vehicle to deliver the antisense ON into the cytoplasm, where the latter could bind to the GFP-encoding mRNA and inhibit the GFP expression. The results were compared to the antisense ON control (transfected by Lipofectamine 2000). The toroidal object induced strong mRNA knockdown and showed reduced cell toxicity compared to the transfected antisense ON control. The presence of the passenger strand was found to be beneficial in improving the recognition specificity of the antisense strand for gene regulations.

The combined use of peptide β sheet formation and DNA duplex hybridization was extended by Ashkenasy et al. to form concentric bilayer nanostructures (Figure 4C).³⁵ An amphiphilic peptide composed of repetitive EF dyads was conjugated to two ssDNAs via the CuAAC reaction. The peptide alone could self-aggregate to form β sheet fibrils, while the two ssDNAs were designed to be complementary to each other. Doping a small amount of two peptide-ssDNA conjugates (1:1 molar ratio) into the amphiphilic peptide stock solution was found to stiffen the fibrils. Increasing the amount of two peptide-ssDNA conjugates (1:1 molar ratio remained) resulted in the spherical structure formation along the fibril skeleton. By pushing the content of two peptide-ssDNA conjugates (1:1 molar ratio was held) to 100%, spherical structures were formed with sizes ranging from 20 to 180 nm. In this case, the free peptide solute was absent in the mixture. These spheres shared an onion-like architecture where the DNA and the peptide layers were arranged in an alternating manner. Both peptide β sheet formation and DNA duplex hybridization contributed significantly to the spherical stability. These spherical nanostructures were explored further as vehicles for encapsulating two model compounds (thioflavin T and doxorubicin [DOX]). The stimuli-responsive release of encapsulated DOX molecules was also investigated. While further research is still needed before applying them for drug delivery *in vivo*, this proof-of-concept work sheds light on assembling peptide-DNA conjugates as potential drug carriers.

Relying on the cooperative synergy between peptide aggregation and DNA duplex hybridization, Yang et al. realized the programmable self-assembly of temperature-responsive nanospheres (Figure 4D).³⁹ A hydrophobic elastin-like polypeptide (ELP) was covalently ligated to each ssDNA via the CuAAC reaction. The chosen ELP could undergo liquid-liquid separation to form coacervates when the peptide solution was heated above the transition temperature. Two pairs of complementary ssDNAs were used; one could form a fully paired dsDNA, while the other had an unpaired ssDNA region for binding to other ssDNAs. As a result, two pairs of peptide-ssDNA conjugates were obtained. When mixing each pair in a buffer solution, stable hollow nanospheres were self-assembled (ca. 55–58 nm in diameter). A bilayer structure was likely formed, where the interior and exterior dsDNA layers sandwiched the middle ELP aggregate region. Both peptide aggregation and DNA duplex hybridization were important for the nanosphere self-assembly. When the solution was heated above the ELP transition temperature, the nanospheres shrank significantly, with their diameters being halved. When the solution temperature was cooled to below

the ELP transition temperature, these nanospheres could restore their original sizes. Further studies showed that most nanospheres could enter HepG2 cells (from human liver cancer cells) through caveolin-mediated endocytosis. Thus, they were also employed as drug carriers to deliver the anti-cancer drug DOX into the target cells.

Reversible superstructured networks were successfully realized by orchestrating three orthogonal interactions, namely aliphatic segment hydrophobic collapse, peptide β sheet formation, and DNA duplex hybridization, in a seminal work from Stupp and co-workers.⁴⁵ These supramolecular architectures are reminiscent of how nature can master non-covalent interactions at the angstrom level to maneuver reversible hierarchical self-assembly of natural proteins at the macroscopic level. A peptide amphiphile was first conjugated to two complementary ssDNA strands via an SPAAC reaction. The resulting two peptide-ssDNA conjugates were then mixed with unmodified peptide amphiphiles in excess for the bottom-up construction of reversible superstructured networks (Figure 5A). The conjugated peptide amphiphile domains self-aggregated with neighboring free peptide amphiphiles through hydrophobic collapse and β sheet formation into long fibers. The remaining hydrophilic ssDNA parts protruded from the fiber surface and bound via Watson-Crick base pairing to their DNA complements anchored on other fibers. Thus, the long peptide amphiphile fibers could further associate with each other to form large micrometer-sized bundles in the hydrogel. Further simulations revealed that such bundle formation could only occur in a very narrow thermodynamic energy window, where (1) the interaction between peptide amphiphiles was strong enough to form stable fibers but weak enough to allow dynamic exchange, and (2) DNA duplex hybridization was strong enough to sustain stable inter-fiber crosslinking: the number of DNA duplex hybridization events should allow sufficient inter-fiber crosslinking bridges while not being so large that the system is kinetically locked (the bundle formation was disabled). When one ssDNA component was extended to an overhang region, adding an invader ON could trigger the dissociation of the hybridized dsDNA via strand displacement. As a result, the bundle formation disappeared. This event could be reversed by adding an anti-invader ON sequence. This unique biophysical property was further employed to explore how cortical astrocytes responded to bundled fibers and individual fibers as two different culture substrates. The ssDNA components were further replaced with peptide nucleic acids and oppositely charged peptide sequences to evaluate their impacts on the bundled fiber formation.

Parallel to the wide use of linear POCs in the self-assembly of infinite nanostructures, Lim et al. observed that cyclic POCs could self-organize to form distinct architectures when compared to their linear counterparts (Figure 5B).⁴² The chosen peptide was equipped with an N-terminal maleimide and a C-terminal alkyne function groups, while each ssDNA sequence had an azide group at the 5' end and a thiol group at the 3' end. The peptide was conjugated to each ssDNA via a Michael addition to afford a linear POC, which was further cyclized via a CuAAC reaction to achieve the wanted cyclic POC. When two cyclic POCs contained complementary ssDNAs, the base-pair interaction between these two ssDNAs was weakened relative to the two linear POC counterparts. This was ascribed to the restrained conformations of both cyclic POCs. Incubation of individual cyclic POCs produced homogeneous spherical aggregates in solution, while the corresponding linear POCs led to a heterogeneous population of fibrous aggregates and spherical micelles. In all formed nanostructures, the peptide domains were stacked in the center, which was shielded by a hydrophilic DNA layer. Doping a second POC containing the

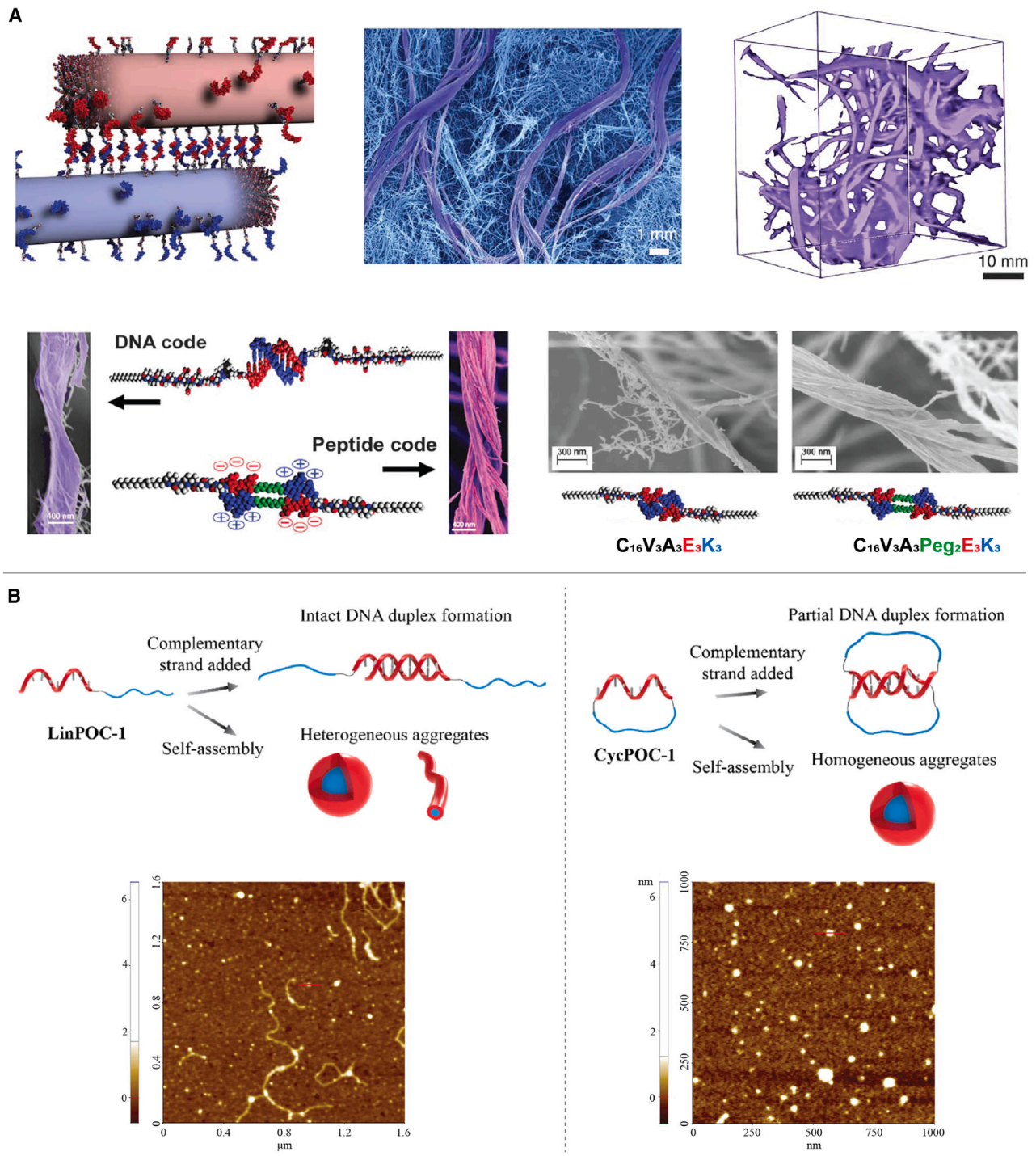


Figure 5. Hierarchical aggregation of peptide-DNA conjugates was programmed via the self-assembly of the DNA domain and/or the peptide domain

(A) Bottom-up construction of reversible hybrid superstructured networks. Adapted with permission from Freeman et al.⁴⁵ Copyright 2018, AAAS.

(B) Cyclic and linear POCs could self-assemble into distinct extended nanostructures. Reproduced with permission from Kye et al.⁴² Copyright 2021, Wiley-VCH.

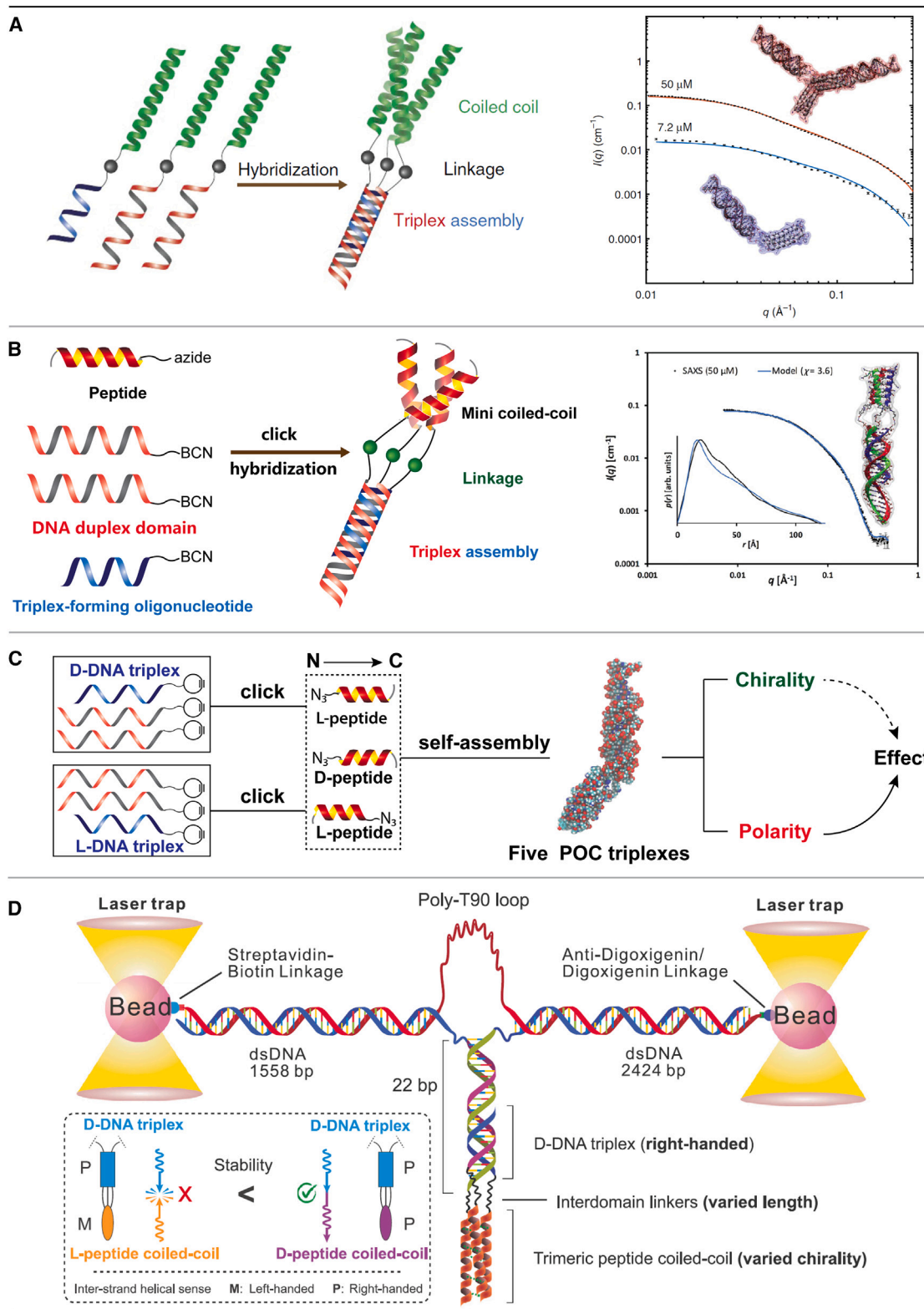


Figure 6. Both the DNA domain and the peptide domain formed finite secondary/tertiary structures in the peptide-DNA conjugate self-assemblies

(A) A peptide trimeric coiled coil was templated by a nucleic acid triple helix. Adaptation from the article by Lou et al.⁴³ is licenced under CC BY 4.0.
 (B) A miniature peptide coiled-coil trimer was scaffolded by the nucleic acid triple helix hybridization. Reproduced with permission from Lou et al.⁴⁴ Copyright 2017, Wiley-VCH.
 (C) Polarity and chirality effects were interrogated between the peptide coiled coil and the nucleic acid triplex domains. Reproduced with permission from Lou et al.⁴⁶ Copyright 2020, Wiley-VCH.
 (D) Chirality transmission was unveiled at a single-molecule level between the peptide coiled coil and the nucleic acid triplex. Adaptation from the article by Pandey et al.⁴⁸ is licenced under CC BY 4.0.

DNA complement could change the self-assembly behavior, which the authors noticed in atomic force microscopy (AFM). Mixing two cyclic POCs produced a loose and less associated structure, whereas two linear POCs self-assembled into a highly dense structure. The authors speculated that the structural difference originated from the weaker base-pairing ability between two cyclic POCs when compared to their linear counterparts. However, reprogramming of early nanostructures, similar to the pathway reported by Stupp and co-workers,⁴⁵ could not be completely ruled out.

Finite secondary/tertiary structures are self-assembled in both DNA and peptide domains

Nucleic acid hybridization and protein topological folding are two highly specific recognition events. Coherently unifying them into a single nanoscale architecture to create the hybrid structure is a formidable challenge. This strategy would not only provide a bottom-up method to use nucleic acid hybridization to manipulate the topological folding of the involved polypeptides (or vice versa) but also open a new chemical dimension in which the power of DNA nanotechnology and peptide nanotechnology could be combined in synergy to enable the assembly of unprecedented functional macromolecules that are impossible with either technique alone. For these purposes, a structural orthogonality is usually required between the nucleic acid secondary/tertiary structure and the protein secondary/tertiary structure. However, designing such two orthogonal macromolecular structures is a challenging task. Pioneering work from Wengel and Jensen and co-workers⁴³ showcased the first example of using a nucleic acid triple helix to facilitate the self-assembly of a peptide trimeric coiled coil, a protein tertiary structure found in 5%–10% of all known protein motifs⁸¹ (Figure 6A). The peptide sequence was derived from CoilV_αL_d (four repeated heptads)⁸² and was predisposed to self-assemble into a mixture of monomer, dimer, and trimer in solution. Three ONs were designed to form a stable triple-stranded helical structure at conditions close to physiological pH and ion strength. Two ONs were hybridized via Watson-Crick hydrogen bonds to form a dsDNA. The third ON could bind via Hoogsteen hydrogen bonds to the major groove of the dsDNA to produce the desirable ON triple helix. Locked nucleic acid thymidine and 5-methyl-2'-deoxycytidine monomers were incorporated into the third ON to impart a high binding affinity toward the target dsDNA. The peptide had an N-terminal azide group, while each ON had a bicyclononyne function group at either 5' end or 3' end. Covalent ligation between the peptide and each ON via the SPAAC reaction afforded three wanted POCs. When mixing these POCs at a near-physiological condition, a nucleic acid triple helix and a peptide trimeric coiled coil were orthogonally assembled. A stabilizing cooperativity was noticed between these two macromolecular domains: (1) the hybridization of nucleic acid triple helix promoted the self-assembly of a stable peptide trimeric coiled coil, and (2) the peptide trimeric coiled-coil formation could reciprocally augment the ON duplex and ON triplex stabilities. Small-angle X-ray-scattering analysis and molecular modeling revealed that the trimeric POC structure existed as a stable macromolecule at a low micromolar concentration, and the solution was homogeneous. When the

concentration was increased to ~ 7 -fold, the trimeric POC structures could further associate with each other to produce a dimer of trimer as the main species. This prototype work revealed the potential of using orthogonal assembly principles such as nucleic acid nanostructures to precisely control the intermolecular folding of multiple peptide strands in a 3D space.

In a follow-up study,⁴⁴ the same research team continued to explore the structural orthogonality between the nucleic acid triple helix and the peptide trimeric coiled coil by removing one heptad unit from the original peptide sequence (Figure 6B). Thus, the new peptide contained only three heptad repeats, and its self-assembling capacity was weakened.⁸² This peptide was conjugated to three ONs (same as in their lead study) via the SPAAC reaction to generate the three wanted POCs. The research objective was to evaluate whether (1) the same nucleic acid triple helix nano-scaffold could template the formation of a short peptide coiled-coil structure and (2) the structural orthogonality was well preserved between the two heteromolecular domains. Please note that the only change the authors made was to shorten the peptide motif by one heptad repeat when compared to those POCs in their lead study. All biophysical measurements were carried out under identical conditions. A miniature peptide coiled-coil trimer was successfully templated by the nucleic acid triple-helix hybridization at the near-physiological condition. Similar cooperative stabilization was noticed between the conjugated macromolecular domains, notwithstanding at a somewhat reduced level. This was rationalized by the miniature peptide coiled-coil trimer being less stable than the four-heptad version and thus having a lower contribution to the cross-domain stabilizing synergy. Interestingly, small-angle X-ray-scattering analysis and molecular modeling showed that the self-assembled POC trimeric structure predominated as separate macromolecules in solution at both low and high micromolar concentrations. This is in a stark contrast to the prior study, where the corresponding POC trimers could further self-assemble into a dimeric form at an elevated concentration. Combining the results, the peptide domain played a pivotal role in this higher-order self-assembly, likely via an intermolecular peptide-peptide interaction, which still needs experimental evidence to confirm.

As a next step, the same team continued to explore whether the polarity of peptide sequence would influence the cross-domain stabilizing cooperativity (Figure 6C).⁴⁶ The three-heptad peptide was used, since no higher-order self-assembly was observed for the corresponding POC trimeric structure.⁴⁴ To invert the sequence polarity, the peptide was designed to have a C-terminal azido function, which was used for conjugation to three cyclooctyne-modified ONs via the SPAAC reaction to produce the wanted POCs. Among the three ONs, two for the DNA duplex formation were identical to those in their preceding work. For the third ON, locked nucleic acid thymidine monomer was replaced with standard thymidine to facilitate the annealing process of nucleic acid triple helix. Accordingly, the experimental pH was lowered to 5.5 to maintain a stable nucleic acid triple-helix formation. By swapping the ON conjugation from the N terminus to the C terminus of the peptide, two POC trimeric structures were self-assembled, where the peptide coiled-coil trimer was linked to the same ON triple-helix scaffold via either the N termini or the C termini. The resulting two macromolecules could be considered as constitutional isomers, despite a minute change for the interdomain linker region. Different stabilizing cooperativities were noticed between these two constitutional isomers, with the N-terminal conjugation being stronger than the C-terminal conjugation. This phenomenon was ascribed to two possible causes: flipped dipole moment of the coiled coil and different local chemical environments when comparing the N terminus to the

C terminus. Meanwhile, the authors also employed unnatural L-DNA, the mirror-image counterpart of natural D-DNA, as artificial nucleic acid scaffolds to template the peptide coiled-coil formation. Relative to D-DNA, L-DNA is resistant to nucleolytic degradation but preserves the same high plasticity and programmability. Likewise, D-amino acids were also used to compose a D-peptide, a mirror-image structure of the above L-peptide that comprised canonical L-amino acids. Therefore, two mirror-imaged peptides were conjugated via the SPAAC reaction to a stereoisomeric pair of six ONs, respectively, providing 12 POCs in total. These POCs were then used to self-assemble four POC trimeric structures (DD, LL, DL, and LD), existing as two stereoisomeric pairs. The experimental results provided evidence for a strong cross-domain stabilizing cooperativity between the peptide coiled-coil trimer and the ON triplex scaffold, which is uniformly present in all four POC trimeric structures. Additionally, all six POC trimeric structures in this study predominated as individual macromolecules in the given buffer condition and no higher-order self-assembling event was observed.

Chirality transmission exists not only in small-molecule asymmetric reactions^{83–85} but also in peptide/nucleic acid secondary structures, including peptide foldamers and DNA double helices.^{86–88} However, such propagation usually demands that the two interacting modalities are located to each other within the van der Waals radii. It remained elusive whether (1) chirality transmission could take place in peptide/nucleic acid higher-order structures and (2) chiral-to-chiral communication was allowed beyond the van der Waals range for these higher-order structures. Benefiting from the knowledge of POC trimeric structures and the ultrasensitive single-molecule mechanical unfolding technique via optical tweezers, Lou and co-workers combined the two laboratories' expertise to explore the chiral-to-chiral communication between the ON triple helix and peptide coiled-coil trimer at a single-molecule level (Figure 6D).⁴⁸ A diastereoisomeric pair of POC trimeric structures were used, where a D-peptide coiled-coil trimer and a mirror-imaged L-peptide coiled coil were conjugated via the N terminus to the same D-ON triple-helix scaffold, respectively. Herein, the D-peptide coiled-coil trimer held the same inter-strand screw sense as that of the D-ON triple helix, whereas the L-peptide one had the opposite inter-strand screw sense. If the proposed chirality transfer did exist, the D-peptide-D-ON combination should be favored over the L-peptide-D-ON combination. All POC components were synthesized using two stereoisomeric peptides and three ONs via the SPAAC reaction following the same bioconjugation strategy developed in the lead work. Each self-assembled POC trimer had two ssDNA regions that were extended from the unconjugated side of the ON duplex and designed to bind to the middle ssDNA regions of a long DNA handle (having a biotin function on one end and a digoxigenin on the other end). The resulting nick positions were ligated to form two perfect DNA duplex arms. A poly-T loop was inserted opposite to the POC trimer structure to confine the dissociated POC strands in proximity to facilitate the re-assembly process. The two ends of the long DNA handle were attached to two beads (one was functionalized with streptavidin and the other with anti-digoxigenin). These two beads were then entrapped by focused laser beams in solution to accomplish the single-molecule setup. A mirror was used to control one bead to move away from the other, inducing the dissociation of the POC trimeric structure. After removing the external force, the POC trimeric structure was self-assembled to the original state, completing a measurement cycle. The repeated cycles produced one or multiple populations of unfolding events from which the rupture forces were measured. For most cases in this study, two unfolding events were obtained: a high-rupture-force event and a low-rupture-force event. The former was assigned to unfolding the POC trimer, while the latter was assigned to the POC dimer, where

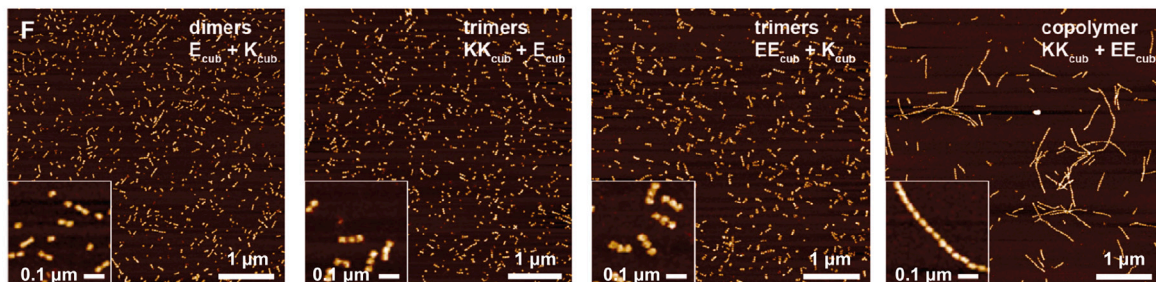
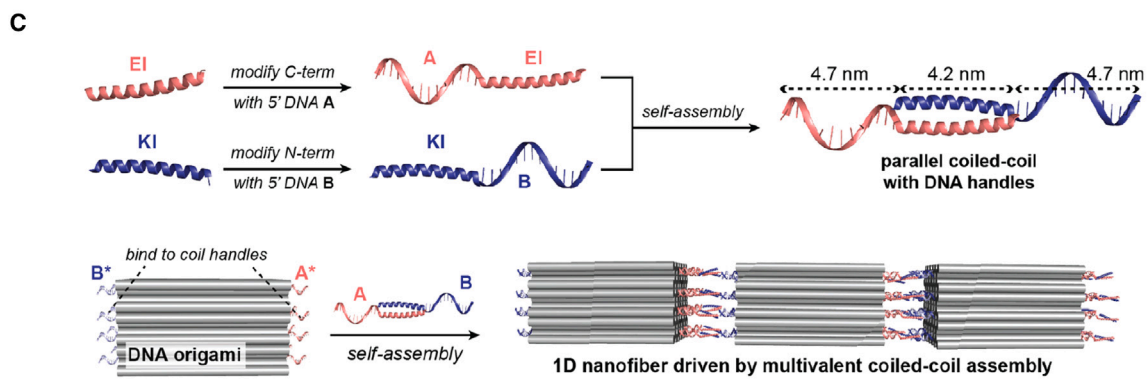
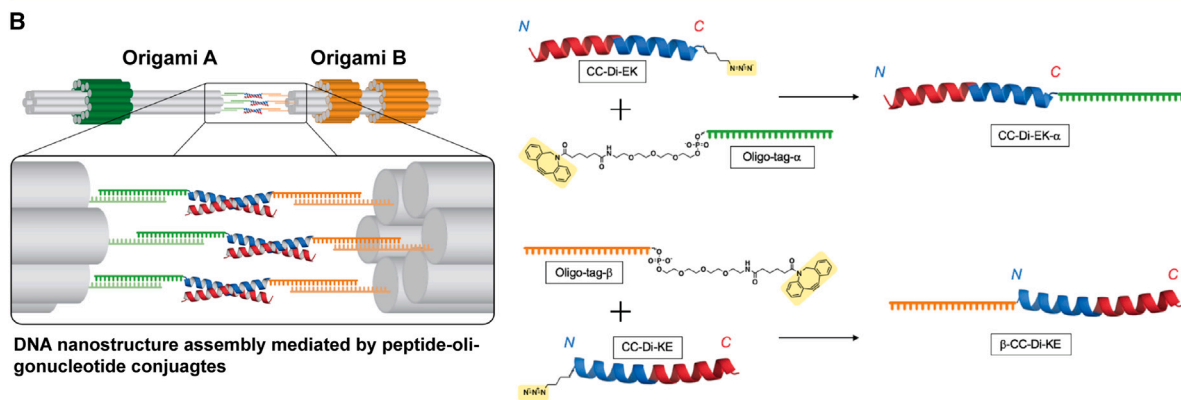
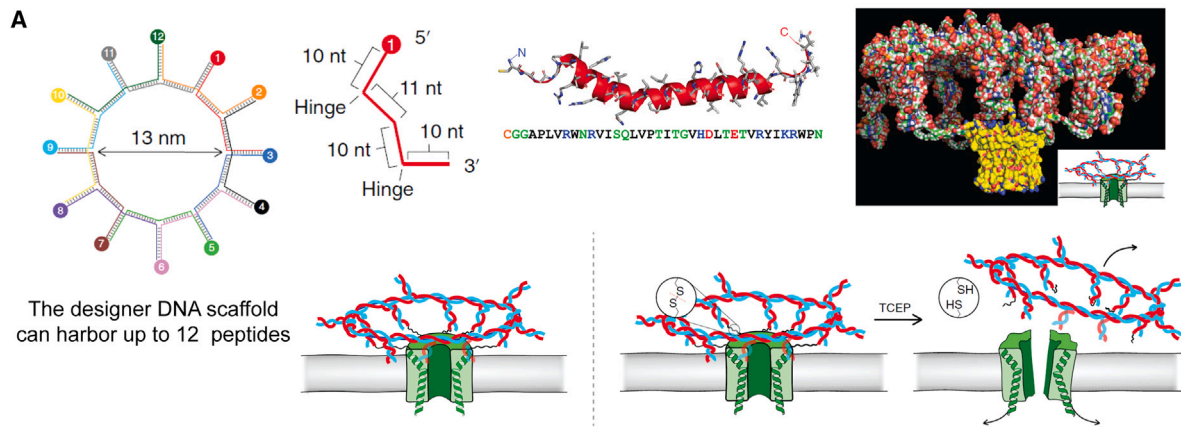


Figure 7. Conjugation of peptides to DNA nanostructures for self-assembly of various nanoscale architectures

(A) Uniform peptide nanopores were templated by a circular DNA nanostructure. Adapted with permission from Spruijt et al.⁶² Copyright 2018, Springer Nature.

(B) DNA origami heterodimer formations could be mediated by a number of peptide coiled-coil dimer interactions. Adaptation from the article by Jin et al.⁵⁹ is licenced under CC BY 4.0.

(C) Controlled self-assembly of cubic DNA origamis into very long nanofibers. Reproduced with permission from Buchberger et al.⁴⁹ Copyright 2020, American Chemical Society.

the third POC binding was prevented. When swapping the L-peptide coiled-coil trimer to the mirror-imaged D-peptide coiled-coil trimer, the rupture forces of the two diastereoisomeric POC trimers were identical. Nevertheless, the corresponding POC trimer population changed significantly. The D-peptide coiled-coil trimer induced a higher POC trimer formation than the L-peptide coiled-coil trimer. This indicated that (1) a chiral-to-chiral communication existed between the mirror-imaged peptide coiled-coil trimers and the D-ON triple helix, and (2) the D-peptide-D-ON combination was favored. The authors then varied the interdomain linker length to explore the effective distance of this new intermolecular force and found it was effective within 4.5 nm, far beyond the van der Waals range. Molecular modeling and small-angle X-ray scattering (SAXS) measurement revealed that the interdomain linker region adopted tightly packed conformations, which likely enabled the chirality transfer between the peptide and ON domains. This study sheds light on an interesting natural phenomenon that neighboring coiled-coil domains are usually folded to have the same screw senses in proteins.

The above-mentioned examples demonstrate that covalent ligation of peptides to ONs leads to a new type of nanoscale building blocks that coherently combine the two highly programmable self-assembly principles into a single macromolecule. The obtained POCs can self-assemble into various architectures ranging from low-nanometer diameters to macroscopic sizes. This was achieved via rational design to fine-tune an elegant balance between the peptide-peptide interactions and the ON-ON interactions. Finite and extended structures can be customized for the peptide domain, for the DNA domain, or both. Diverse applications have been explored for these prototype hybrid architectures, including drug delivery, controlled release, stimulated neural cell response, *de novo* protein design, and new intermolecular force discovery. Although it has slowly emerged in the last few years, the POC nanotechnology is expected to boom in the next decade to offer the scientific community a powerful molecular tool, complementing the current nanotechnological arsenal.

Oligopeptides/polypeptides conjugated to DNA nanostructures as building blocks

Membrane-spanning protein nanopores regulate transport across cellular membranes. They have also found important applications in nanomedicine,⁸⁹ DNA sequencing,⁹⁰ and single-molecule analysis.^{89,91} Most widely used protein nanopores can readily self-assemble and insert into the membrane with given pore sizes.^{92–98} However, it remained a grand challenge to engineer individual peptides to assemble uniform nanopores with arbitrarily predefined sizes and controlled permutations of peptide display. To address this challenge, Bayley and co-workers designed a circular DNA nanostructure to harbor a defined number of amphiphilic peptides to form uniform nanopores in planner lipid bilayers (Figure 7A).⁶² The amphiphilic peptide used here derives from the D4 domain of octameric polysaccharide transporter Wza and is used by *Escherichia coli* to form protein nanopores in its membrane for extracellular polysaccharide transportation. The amphiphilic peptide was unable to form stable open pores by itself.⁹⁶ Twelve short DNA sequences were used to assemble the desirable circular DNA scaffold in a diameter of 13.6 nm.

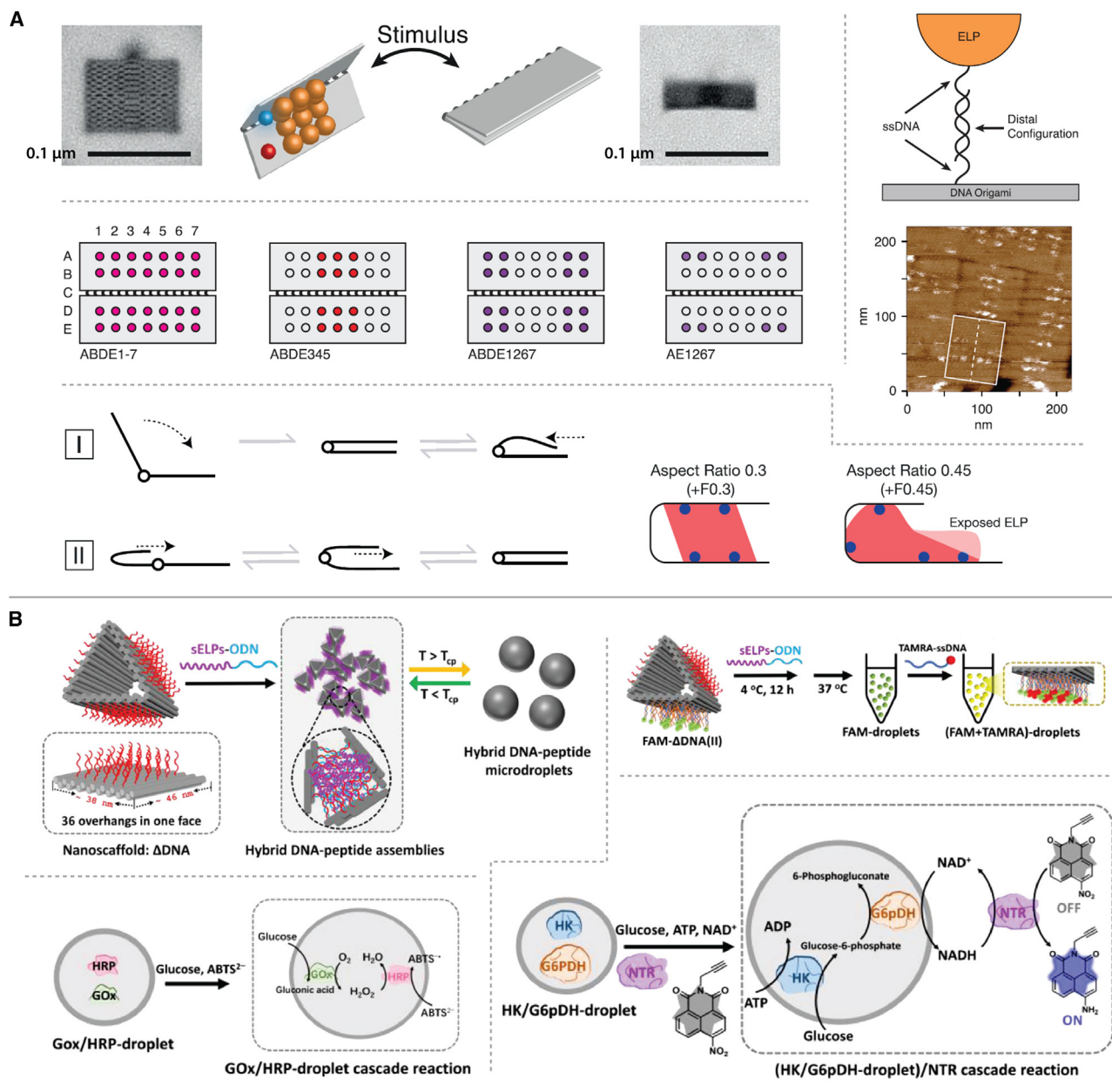
Twelve dsDNA arms pivoted around the circular rim, which were used to anchor a different number of amphiphilic peptides. Each DNA sequence had an amino function group at the 5' end, while the amphiphilic peptide contained a cysteine residue at the N terminus. The covalent ligation between 12 DNA components and the amphiphilic peptide was completed via a hetero-bifunctional molecule called succinimidyl-[(N-maleimido-propionamido)-diethyleneglycol] ester. As a result, 12 POCs were obtained. The controlled permutations of peptide display were realized by mixing the POCs (x) and unmodified DNA sequences (12-x) to assemble the circular DNA scaffold. Only when eight POCs were mixed with four unmodified DNA sequences could the self-assembled nanostructure readily insert into the planner lipid bilayers to form an artificial nanopore, and it remained stable for extended periods. The resulting nanopore could be kept in an open state for multiple hours once a high-conductance state was reached at the given applied potentials. No stable nanopore could be formed when the DNA circular scaffold harbored fewer than eight peptides. If more than eight peptides were involved, nanopores could be formed but only expressed the same conductance as the peptide octamers. The DNA circular scaffold played a vital role in pre-organizing the eight anchored amphiphilic peptides; a complete loss of nanopores was observed 2 min after removing the DNA circular scaffold. Interestingly, no stable pore formation was noticed when the conjugation site was changed from the N terminus to the C terminus of the amphiphilic peptide. This study paved an avenue toward the bottom-up construction of uniform large nanopores templated by self-assembled DNA for various chemical and biological applications.

Conversely, the peptide self-assembly principle can also be used to promote the association of two DNA nanostructures. The more peptide-peptide recognition events are involved, the stronger binding is expected between the two DNA nanostructures, whereby the dissociation constant can be estimated for the individual peptide self-assembly module. When multiple peptide-peptide interactions are designed at the interface, the actual state of polyvalency can be deconvoluted, which otherwise would be impossible to measure. Woolfson and co-workers employed a neutral peptide coiled-coil parallel heterodimer as the peptide self-assembly principle to join two DNA nanostructures (Figure 7B).⁵⁵ The two peptides were designed to have four heptad repeats, where an asparagine residue was incorporated every two heptad repeats to inhibit unwanted homodimer formation. One peptide had an azido group at the N-terminal residue, while the other had it on the C terminus. These two peptides were then clicked to two DBCO-modified ONs via the SPAAC reaction, respectively. As a result, two POCs were obtained. Herein, the ON domains of the two POCs could hybridize to the ssDNA handles extended from two DNA origami nanostructures. Two readily distinguishable origami nanostructures were assembled; one had a single sleeve wrapped around the central six-helix bundle, while the other had two sleeves. This design allows the rapid determination of individual origami monomers in electronic micrographs. Each DNA origami nanostructure had either one, two, or three ssDNA handles protruding from one end. When incubated with the corresponding POCs, the DNA Watson-Crick pairing between the ssDNA handles and the POCs led to the predefined peptide display on each DNA origami (one, two, or three peptides). Upon mixing two complementary DNA origami monomers, they could associate through the peptide coiled-coil self-assembly. DNA origami heterodimers were rarely observed by transmission electron microscopy (TEM) when there was only one peptide for each origami monomer. The K_D value (130 ± 20 nM) derived from the single-peptide display was in good agreement with the one (102 ± 26 nM) determined from two free peptides in solution. When each origami monomer had two peptides, the K_D value (25 ± 3 nM) decreased

only five times, implying that a single-peptide coiled-coil heterodimer was formed between the two origami monomers. The small improvement was ascribed to the 4-fold increase in possible contacts between two pairs of peptides to form a single coiled-coil heterodimer. When both origami monomers had three peptides, the K_D value (0.7 ± 0.1 nM) was reduced by nearly two orders of magnitude relative to the single-peptide display. This strongly suggested multiple peptide-peptide interactions occurred between the two origami monomers: at least two peptide coiled-coil heterodimers persisted simultaneously. This work offered a new method to explore the real state of polyvalent interactions between nanostructures and may inspire the development of more sophisticated peptide-DNA hybrid architectures for various nanotechnological applications.

Peptide coiled-coil recognition could also serve as a main drive for the hierarchical assembly of DNA origami nanostructures. Stephanopoulos and co-workers combined peptide coiled-coil dimerization and DNA duplex hybridization to program the self-assembly of a cubic DNA origami to form very long nanofibers (Figure 7C).⁴⁹ The two peptides (EI and KI) could form a stable parallel heterodimer via specific hydrophobic and electrostatic interactions ($K_D < 0.1$ nM), which was essential to direct the DNA origami self-assembly. One peptide contained an N-terminal azide group, while the other had the azide at the C terminus. To bridge the peptide coiled-coil dimer and the DNA origami cuboid, two 14-mer ONs were employed. Each ON was furnished with a DBCO moiety at the 5' end and could hybridize to the ssDNA region extended from the DNA cuboid. The peptide-ON conjugation was accomplished via the SPAAC reaction to produce two wanted POCs as the connection module. Both ends of the DNA origami cuboid were extended to have 1–12 ssDNA handles, which could hybridize to the ON domains of the two POCs. Different ssDNA sequences were used for the two ends. The 1D DNA origami arrays were first explored by a one-pot assembly pathway to anneal all component strands of the DNA origami cuboids and the two POCs at the same time. The DNA cuboid having eight ssDNA handles at each end was found to form the desirable DNA origami arrays most efficiently. The authors used such origami cuboid design to explore a further two hierarchical assembly strategies to improve the efficiency of the wanted nanofiber formation. Both were carried out as a two-step procedure, where the DNA origami cuboids were always annealed at the first place. In the first sequential assembly pathway, the DNA origami cuboid was self-assembled with each POC separately, and the resulting two monomers were used for nanofiber growth. A similar efficiency was observed relative to the one-pot assembly pathway. In the second sequential pathway, the authors purified the DNA origami cuboid via spin filtration before the incubation with the preformed POC dimer (via coiled-coil interaction). This method significantly increased the efficiency of nanofiber formation and had their lengths reach up to a few micrometers. This research opened immense possibilities to design and assemble various hybrid peptide-DNA nanostructures with added functions. More recently, the research team advanced the complexity of the hierarchical assembly by adding two extra chemical layers: (1) a monomeric protein, known as the 10th type III Fn domain, which served as a bridging unit to connect the hybrid DNA-peptide modules, and (2) a second pair of peptides (P3/P4), orthogonal to the KI/EI pair used in the lead work, which could self-assemble to form another parallel coiled-coil heterodimer.⁹⁹ When the resulting protein-DNA nanofibers were coated on the glass surface, they were found to preserve the protein biological functions of binding to integrins and promoting cell adhesion/spreading.

In the above examples, relatively short peptides (tens of amino acid residues) were used for the peptide self-assembly principle. Parallel to those works, the interactions



between long peptide sequences were also explored to direct the topological folding of DNA nanostructures. Pirzer and his team used a series of ELPs ranging from 119 to 343 amino acid residues for the peptide module.³⁷ Those long peptides had two different molecular states, a hydrophilic state and a hydrophobic state, which existed under different chemical conditions. Thus, by changing the temperature and/or chemical conditions, they could undergo a fully reversible hydrophilic-hydrophobic phase transition to form stimuli-responsive peptide assemblies. This

unique property was employed to reversibly close and open the two leaves of a butt-hinge-like DNA origami nanostructure (Figure 8A). Two types of ELPs were used in this study, a canonical (GVGVP)₄₀ peptide, and three others mixed by the canonical motif (GVGVP) and the non-canonical motif GVGAGVP. The latter type was only used to evaluate whether different ELP lengths could influence the controlled folding of the DNA origami nanostructure. When the temperature or the salt concentration crossed the thresholds, both types of peptide could transform from relaxed water-solvated states to collapsed hydrophobic states (β -spiral).¹⁰⁰ Each peptide was modified at the N-terminal residue to have an azido group, which was conjugated to the alkyne-modified 21-mer ON via the CuAAC reaction to generate the four wanted POCs. The butt-hinge-like DNA nanostructure was assembled via the DNA origami technique. From both leaves of the butt-hinge-like DNA nanostructure, a predefined number of ssDNA handles (1–12) was extended from the same side, which readily hybridized to the 21-mer ON domain of the POCs. As a result, the peptide-actuated dynamic DNA nanodevices were assembled. The topological folding of the DNA nanodevices was found to be concentration independent, probably due to the intra-structural transformation nature. The temperature cycle between 10°C and 40°C showed that the two leaves of the butt-hinge-like DNA nanostructure could open and close reversibly. Increasing salt concentration (from 0.5 to 3.0 M NaCl) could lower the transition temperature and thus promote the closed state of the two hinged leaves. Possible dimerization between two separate nanodevices was explored by TEM. Despite apparent background noise (20%–30%, also for the negative control), the positive control gave a 90% yield of the dimer formation. Thus, the authors concluded that intra-structure folding was strongly favored over inter-structure dimerization. Additionally, the ELP length was found to be inversely related to the transition temperature: the shorter the ELP length, the higher the transition temperature of the peptide. In this study, three different conformations were observed for the two leaves of the butt-hinge-like DNA nanostructure: (1) a fully open state, (2) a fully closed state, and (3) a partially closed state. The ratio of two closed states for a given peptide-actuated dynamic DNA nanodevice was determined by the ELP length and how ELPs were displayed on the two hinged leaves. This research work may pave an avenue toward the construction of advanced responsive dynamic DNA devices and automated hybrid peptide-DNA molecular machines.

More recently, taking advantage of its temperature-triggered phase separation behavior, Yao et al. used a much shorter ELP (sELP) to program the reversible inter-structure assembly of a DNA triangular prism at a macroscopic scale (Figure 8B).⁴⁰ The DNA triangular prism (ca. 46 × 38 × 38 nm) was assembled through the DNA origami technique. The three outer faces were extended to have a predefined number of ssDNA handles (same sequence), with 36 handles on a single face, 72 handles on two faces, and 108 handles on all three faces. Thus, three DNA origami nanostructures were composed to harbor different numbers of ELPs. A 30-mer sELP, (VPGFG)₆, was used for this study, and the peptide was modified to have a C-terminal alkyne function. This peptide was conjugated to an azido-bearing ON (18-mer) via the CuAAC reaction to produce the wanted POC. The latter ON was complementary to the ssDNA handles on the outer faces of the DNA origamis. Three DNA origami monomers were produced upon POC binding, with the sELP display on one face, two faces, and all three faces. Below the phase transition temperature, only intra-structure folding was observed for the one-face sELP display and the individual DNA origami monomers were dispersed in the buffered solution (4°C). This is reminiscent of the intra-structure folding of a butt-hinge-like DNA nanostructure by Pirzer and his team (*vide supra*).³⁷ In contrast, both two-face sELP display and

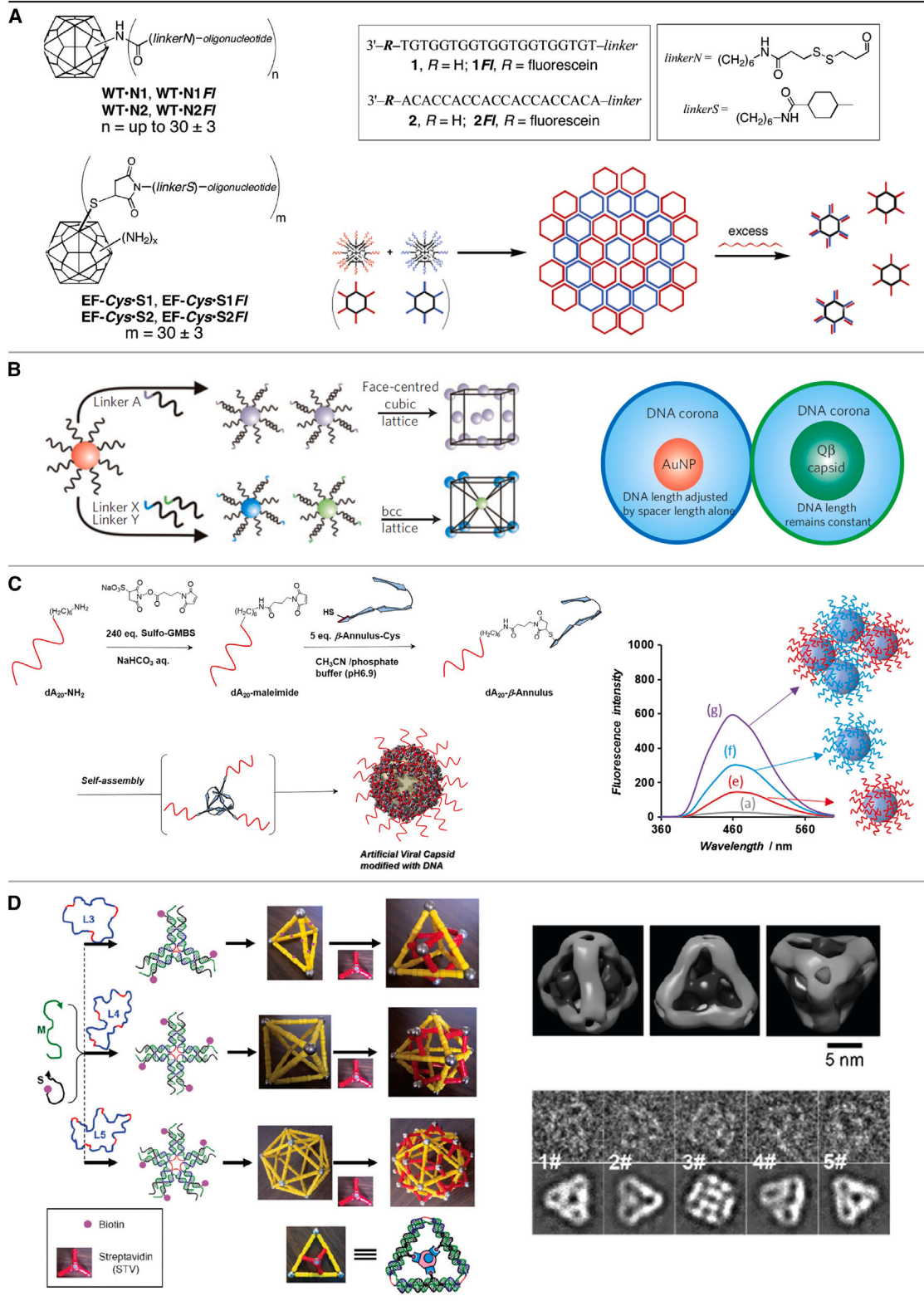


Figure 9. Conjugation of ONs to proteins for assembling various hybrid nanostructures

- (A) The self-assembly of CPMV was directed by DNA duplex hybridization. Adapted with permission from Strable et al.³³ Copyright 2004, American Chemical Society.
- (B) Alloy lattice structures were assembled using a virus-like protein particle and AuNPs. Adapted with permission from Cigler et al.⁴¹ Copyright 2010, Springer Nature.
- (C) Self-assembly of artificial viral capsids by POCs composed of a synthetic β -annulus peptide and ONs. Reproduced with permission from Nakamura et al.⁶³ Copyright 2017, Wiley-VCH.
- (D) 3D protein organizations could be directed by DNA polyhedral scaffolds. Reproduced with permission from Zhang et al.⁶⁶ Copyright 2012, Wiley-VCH.

three-face sELP display led to the formation of aggregation-like large structures, whereas the solutions remained as one phase (4°C). Therefore, the authors continued the research by focusing on the two- and three-face sELP displays. The phase transition temperature was found to be concentration dependent: the more concentrated the solution was, the lower the phase transition temperature of the DNA origami monomer. The two- and three-face peptide displays had similar phase transition temperatures. When the solutions were heated to above the phase transition temperature, both two- and three-face sELP displays could induce the formation of uniform spherical microdroplets (~1.2 μm) in the same buffered solution (37°C). A photo-bleaching experiment confirmed that the formed microdroplets possessed a liquid-like property and were accessible for guest molecules. The repeated temperature cycle between 4°C and 37°C confirmed the reversibility of microdroplet formation. The real-time observation by confocal laser scanning microscopy showed that the microdroplets were formed in tens of seconds. The authors then utilized these microdroplets as open “microreactors” to host two cascaded enzymatic reactions. The two-face sELP display was used here. The remaining face of the DNA origami monomer was modified to have two orthogonal ssDNA handles, readily hybridized to two complementary ONs conjugated to two different enzymes. Two different pairs of enzymes were employed: glucose oxidase/horseradish peroxidase and hexokinase/glucose-6-phosphate dehydrogenase. The latter pair was designed to cooperate with nitroreductase in solution to induce a chain of three enzymatic reactions. The microdroplet states performed better than the corresponding dispersed states and free ON-conjugated enzyme controls. This was ascribed to the molecular crowding effect and the reduced diffusion barrier in the liquid-like microdroplets. The proposed concept in this work may inspire the development of advanced peptide-DNA hybrid machines and life-inspired materials.

Protein-conjugated ONs as nanoscale bricks

In this section, we summarize the recent milestones where large protein structures were used for the peptide domain. The covalent conjugation between protein structures and short ONs has provided a number of nanoscale building blocks for different chemical and nanotechnological applications. This concept was pioneered by Finn and co-workers, demonstrating that the DNA duplex hybridization event could be employed to direct the assembly of an icosahedral virion (Figure 9A).³³ The authors used the cowpea mosaic virus (CPMV) in this study. CPMV had an icosahedral assembly of 60 identical coat proteins, and the viral capsid was formed with a diameter of 30 nm. Each coat protein comprised two subunits, a small domain (24 kDa) and a large domain (42 kDa). In the wild-type CPMV, the small domain had a reactive lysine residue, which was used for covalent conjugation of two complementary 20-mer ONs (carrying an active carboxylate ester) via the NHS-ester chemistry to produce two desirable CPMV-ON conjugates. Half of the available lysine residues could be functionalized with the ONs, reaching a level of 30 ± 3 ONs per virion. Experimental evidence supported that the two CPMV-ON products had intact viral particles. Additionally, the Watson-Crick base-pairing capacity was well preserved for the attached ONs. By mixing the two CPMV-ON products, light

scattering and TEM experiments showed that an immediate virion aggregation was observed. This self-assembly process could be reversed by adding the excess of either ON alone. When the CPMV domains were respectively labeled by two different fluorescent dyes (fluorescein and rhodamine), fluorescence resonance energy transfer (FRET) experiment indicated that the ON hybridization could bring a decent population of two virion-anchored fluorescent dyes in proximity (<5.5 nm). TEM analysis showed that the annealing temperature could influence the virion aggregation pattern significantly. When the two CPMV-ON products were annealed at 4°C, small aggregates were induced in a two-dimensional (2D) hexagonal packing. When increasing to room temperature, large 2D arrays were formed. When the temperature was further increased to 35°C–40°C, 3D arrays were produced. The different virion aggregation patterns were ascribed to the repeated TGG/CCA nature of the two employed ON sequences. At low temperatures, short ON duplexes could form as kinetic products, leading to the formation of less extensive and weaker arrays. These arrays could easily be broken up on the TEM grid during the sample preparation; thus, only small aggregates or 2D arrays were observed. At a high temperature, the short ON duplex formations were inhibited, and the balance was shifted to favor the longer and more thermodynamically stable ON duplex. The resulting 3D arrays were well preserved on the TEM grid. When heating these large arrays to 45°C, they rapidly dissociated to separate CPMV-ON monomers, showing a maximum ON duplex length (11 base pairs [bp]) that could be formed between the two neighboring virions. A mutant-type CPMV was also involved, where a cysteine-alanine di-residue was engineered into the large domain of the viral coat protein. The cysteine residue was designed for covalent conjugation with the same two ON complements (carrying a maleimide function) via the Michael addition. Similar virion aggregation phenomena were observed.

Park and co-workers explored using the DNA duplex hybridization event to assemble two completely different core particles, an organic virus-like protein particle and inorganic gold nanoparticles (AuNPs), into two well-defined alloy lattice structures (Figure 9B).⁴¹ The icosahedral bacteriophage Q β capsid was chosen as the model protein particle due to its stability, monodispersity, and surface addressability. The capsid comprised 180 identical proteins and had a diameter of ca. 28 nm. Each protein unit had four free amino groups on the outer surface, which were treated with an azido-bearing linker containing an NHS-ester group at the opposite end to furnish the click handles. The ON sequence was designed to have an alkyne function at the 5' end. The covalent ligation between the Q β capsid and the ON sequence was accomplished via the CuAAC reaction to afford the desirable Q β -ON conjugate. For the AuNPs, four different sizes were used (10, 15, 20, and 30 nm in diameters). An orthogonal ON sequence was attached to the AuNP surfaces through the gold-sulfur linkage. With the help of three auxiliary ONs, the Q β capsid and the AuNPs were glued together via the DNA duplex hybridization event. By actuating the lengths of two auxiliary ONs, a similar interparticle distance (44.9–48.0 nm) could be maintained between the Q β capsid and the four different AuNPs. When the AuNP size was increased from 10 to 20 nm, finite NaTl-type alloy lattices were self-assembled with very similar features. The experimental results were consistent with the theoretical calculations. When the AuNP size was further increased to 30 nm, a cesium chloride-type alloy lattice was observed. This indicated that, besides the interparticle DNA duplex hybridization event, the direct core particle contacts also contributed to determining which alloy lattice was formed. The DNA-controlled assembly of heterogeneous core particles to generate different alloy lattices may open the door to creating tailored hybrid materials for photonic crystal applications.

The ON conjugation to the viral coat protein unit could also be accomplished prior to the self-assembly of the viral capsid. It was found to be innocuous for the latter process. Matsuura and his team used a synthetic 24-mer β -annulus peptide derived from the capsid protein unit of tomato bushy stunt virus to demonstrate the applicability (Figure 9C).⁶³ This peptide could self-assemble into artificial viral capsids (ca. 53 nm in diameter in dynamic light scattering [DLS]) at neutral pH, with its C terminus being located at the capsid outer surface. Thus, the authors inserted a cysteine residue near the C terminus of the peptide for ON conjugation. Two 20-mer ON sequences were used, dT₂₀ and dA₂₀, each containing an amine function group at the 5' end. The ONs were reacted with the activated ester of a hetero-functional linker to furnish a maleimide group at the 5' end. The covalent conjugation between the β -annulus peptide and the two ONs were completed via the Michael addition reaction, producing two POC building blocks. Like the unconjugated β -annulus peptide, both POC could self-assemble to form artificial viral capsids. The resulting hybrid nanospheres had increased diameters, probably due to the extra ON layer on the capsid surface. These hybrid nanospheres preserved the Watson-Crick base-pairing ability with complementary ssDNA strands. The DNA duplex hybridization events could induce significant capsid aggregation. Large capsid aggregates were also observed when mixing two hybrid nanospheres modified with the complementary ONs. Considering the empty interiors of hybrid nanospheres, this study may inspire the development of more advanced DNA-functionalized artificial viral capsids for targeted delivery and tailored immunotherapy.

The high surface addressability of DNA nanostructures was explored to engineer protein displays in a precise manner. Mao and his collaborators exemplified that symmetric DNA polyhedra could serve as ideal nano-scaffolds to direct 3D protein organization (Figure 9D).⁶⁶ Three DNA polyhedra were used in the study, namely tetrahedron, octahedron, and icosahedron. They were self-assembled from three different star-shaped DNA building blocks following the method developed by the same authors.^{101–103} In the resulting DNA polyhedral structures, each triangle face was designed to have three protein-binding sites, one on each triangle side. The biotin function was incorporated into the DNA polyhedron as the protein-binding sites, whereby streptavidin could be immobilized onto each triangle face via the strong and specific biotin-streptavidin interaction. In this case, all three biotins were bound to the streptavidin molecule. The streptavidin corona was successfully decorated onto each DNA polyhedron surface, as shown by gel electrophoresis, AFM, and cryogenic electron microscopy (cryo-EM). The streptavidin binding on the surface could also influence the DNA polyhedral scaffolds both mechanically and thermodynamically. Taking the DNA tetrahedron as an example, the streptavidin binding not only induced a local DNA strut distortion but also imparted increased stability to the core nano-scaffold. To demonstrate the generality of the proposed strategy, the authors employed the DNA tetrahedron to tailor a 3D antibody display via a specific antigen-antibody interaction (fluorescein and anti-fluorescein antibody). Each triangle face of the DNA tetrahedron was modified with three fluorescein molecules, two of which could bind to a single antibody simultaneously. The resulting nanostructures resemble many virus structures (nucleic acids were encapsulated by multiple copies of coat proteins). Strong immune responses are expected to be induced if multiple antigens are displayed on a single nanostructure. Therefore, this concept could be used for the development of potent vaccines. Moreover, when the biotin/fluorescein used in this study is replaced by aptamers, the proposed strategy can be further extended to organize a wide range of ligands.

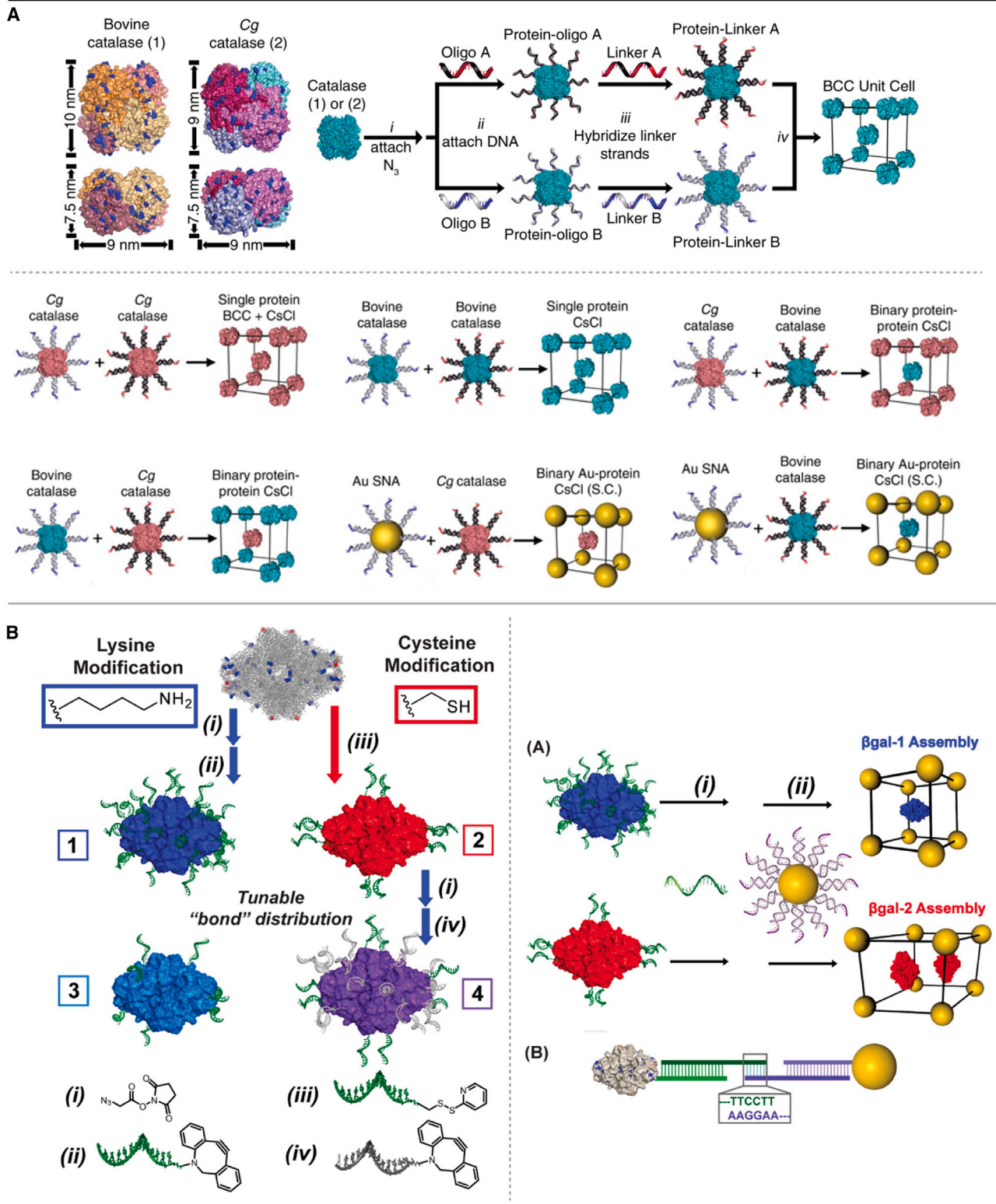


Figure 10. ON display on the protein surface could be used to program different types of crystal unit cells

(A) Two distinct proteins self-assembled into superlattices in the drive of DNA duplex hybridization. Reproduced with permission from Brodin et al.⁵⁰ Copyright 2015, National Academy of Sciences.

(B) Different superlattice types could be formed when ONs were conjugated to the protein surface at distinct locations. Adapted with permission from McMillan et al.⁵¹ Copyright 2017, American Chemical Society.

Developing a general strategy to assemble different proteins into a preconceived lattice was a difficult task. The ideal outcome was that all confined protein components in the given superlattice can retain their native functionalities. When combined with inorganic nanoparticles, functional hybrid crystalline materials could be fabricated in a bottom-up manner. This idea was realized by Mirkin and his team by using the DNA duplex hybridization event to direct two model proteins to self-assemble into superlattices (Figure 10A).⁵⁰ Both model proteins were tetrameric heme-containing enzymes, bovine catalase and *Corynebacterium glutamicum* (Cg) catalase. Each catalase was modified with a different ON strand, and the catalase-ON conjugation was completed in two steps. The amine groups on the catalase surface were firstly reacted with the activated acyl group of a hetero-functional linker to impart the wanted azido groups. The resulting catalases were then conjugated to the respective ON strands (each had a DBCO function at the 5' end) via the SPAAC reaction to afford the desirable POC products. The dense DNA coating over the catalase surface did not perturb the inherent enzymatic activity to catalyze the H₂O₂ disproportionation. The obtained POC products were then used to assemble single-protein lattices and binary protein-protein lattices with the help of two auxiliary ON strands to mediate the inter-protein-DNA duplex hybridization. A slow annealing process was employed to ensure the production of the most thermodynamically stable state. The single-protein lattice assembled from Cg catalase was predominantly arranged in the body-centered cubic type. Interestingly, the lattice from bovine catalase alone and binary protein-protein lattices were found to be characteristic of the cesium chloride type. The authors further replaced one catalase of the binary protein-protein system with an AuNP (similar size to catalases) to construct two hybrid AuNP-protein superlattices. These AuNPs were each modified with ON strands via the gold-thiol bonds. When the AuNP and the catalase were co-assembled via the same DNA duplex hybridization, the resulting binary AuNP-protein lattices also adopted the cesium chloride type. This was in stark contrast with the authors' earlier results that the identical AuNPs induced the body-centered cubic-type lattices upon inter-nanoparticle DNA duplex formation. The differences were ascribed to the shape anisotropy and the nonuniform surface chemistry of two model proteins used for this study. The single crystals formed by Cg catalase alone were capable of decomposing H₂O₂, but its catalytic activity was reduced by ca. 20-fold when compared to the free Cg catalase. The enzymatic activity was well preserved after five rounds of cycles upon catalysis and the Cg catalase crystal lattice remained intact. This research may pave the avenue toward programming the self-assembly of various functional biomaterials.

In a follow-up study, the same research group explored whether the ON-conjugation landscape on the protein surface could influence the superlattice type (Figure 10B).⁵¹ The tetrameric β -galactosidase (β gal) was chosen as the model protein, which could hydrolyze the β -glycosidic bond of galactose. The β gal surface was functionalized by the same ON sequence to have a uniform ON corona or locally clustered ON modifications. Similar to the method developed in their lead work,⁵⁰ 36 solvent-accessible amines (evenly distributed) of the β gal surface were converted into the azido function using a hetero-functional linker (containing an NHS ester and an azide). The obtained intermediate was then reacted with the 5'-DBCO-modified ON to furnish a homogeneous ON corona. In parallel, eight cysteine residues at the four

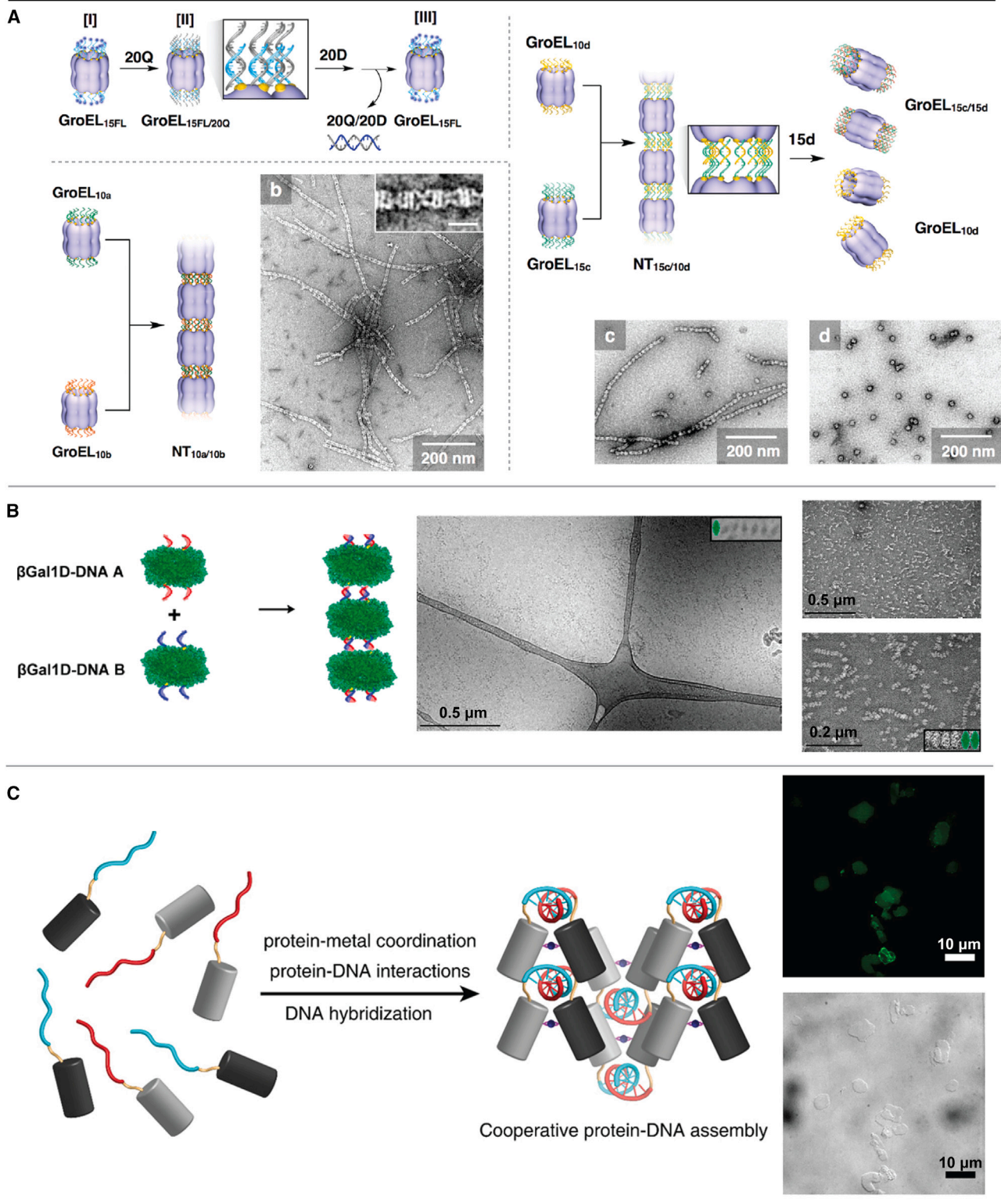


Figure 11. Continued

(B) Two DNA duplex hybridization events were enough between neighboring protein monomers to drive the formation of 1D wire-like protein polymers. Insets show cartoon of protein along its 17 × 8-nm face. Adapted with permission from McMillan et al.⁶⁰ Copyright 2018, American Chemical Society. (C) Three different non-covalent interactions (protein-protein interaction, ON duplex hybridization, and ON-protein interaction) were orchestrated to assemble nucleoprotein-like architectures. Adapted with permission from Subramanian et al.⁶¹ Copyright 2018, American Chemical Society.

vertexes of the protein were used for ON conjugation via the thiol-disulfide exchange reaction. Four locally clustered ON modifications were generated on the protein surface. The ON conjugation to the protein surface did not impair the βgal catalytic activity in both cases. With the help of two auxiliary ON strands, the obtained two POC products were individually co-assembled with an AuNP (10 nm in diameter, functionalized by ONs via gold-thiol bonds) in a similar fashion to their lead work.⁵⁰ When the ON strands were evenly distributed on the βgal surface, a cubic superlattice was formed in the cesium chloride type. In contrast, while the ON strands were locally clustered on the βgal surface, a hexagonal superlattice was assembled in an AB₂ packing arrangement (βgal/AuNP = 1:2). Interestingly, when the authors reduced the conjugated-ON strands but kept their random distribution pattern, two different types of arrangements were observed: disordered aggregates and ordered domains. The latter were assembled through a hexagonal superlattice and densely packed in the AB₂ structure. The experimental results revealed that two main factors could influence the hybrid crystal unit cell formation: the number of ON strands conjugated on the βgal surface and the location of the ON-βgal conjugation. This study may inspire the bottom-up construction of novel multicomponent materials for catalysis and sensing applications.

The DNA hybridization strategy was explored to assemble responsive 1D protein nanotubes (Figure 11A).⁵⁹ Aida et al. employed a tetradecameric barrel-like chaperone (GroEL) as the protein domain, of which the two apical domains were engineered to have a certain number of accessible cysteine residues. The maleimide-modified ONs were reacted with the protein via Michael addition to furnish the ON sequences on the two open sides of the barrel-like protein (ideally 14 + 14 ON strands). Two pairs of 10-mer complementary ONs were used, whose melting temperatures were well below the protein denaturation temperature. Such design was to preserve the intact protein conformation during the ON duplex annealing process. Therefore, two pairs of POCs were produced. By annealing either of two POCs in a 1:1 M ratio, the ON hybridization events led to very long protein nanotube formations. Both the annealing temperature and the 1:1 equivalent of two POC species were found to play an indispensable role in generating protein nanotubes with small polydispersity. The protein apical domains were found to be slightly crooked in the protein nanotubes, probably due to the mechanical shear applied by the multivalent ON duplex formations. In the next step, a fifth POC was designed to have a 15-mer ON domain, which could hybridize to one of the above 10-mer ONs but leave an unpaired 5-mer toehold region. When the two POCs were properly mixed, the inter-protein ON hybridization events (between the 15-mer ON and the 10-mer ON) led to a similar protein nanotube formation. Adding the 15-mer ON complement could dissociate the protein nanotubes via strand displacement (mediated by the 5-mer toehold region). As a result, two POC monomers were formed, one having a 15-mer ON duplex and the other having a 10-mer ON strand. Such stimulated protein nanotube disassembly was found to be highly specific, orthogonal to the parental protein nanotubes that lacked the 5-mer toehold region. The authors surmised that other DNA/RNA modalities could be integrated to give the hybrid protein nanotubes tailored functions applicable for biological cue sensing and targeted delivery.

The 1D wire-like protein polymers could be self-assembled via only two DNA duplex formations between neighboring protein monomers (Figure 11B).⁶⁰ The concept was proposed by Mirkin and his team. A D2 symmetric, tetrameric β gal was chosen as the model protein. This protein was also utilized by the same authors to construct two different classes of protein-AuNP superlattices (*vide supra*).⁵¹ The protein surface was scrutinized to identify a suitable position for ON conjugation. The 265th position, where a threonine residue was originally located, was recognized as the optimal ON anchoring site near the subunit interface. A rationally designed β gal variant was thus expressed, of which all solvent-accessible cysteine residues were mutated to serine and the threonine residue at the 265th position was replaced with a cysteine. Upon ON conjugation, each protein subunit would carry one ON strand. The resulting tetrameric β gal variant would have two pairs of ON strands that were symmetrically anchored on the two opposite protein surfaces. The distance between the two ON strands on the same protein surface was ca. 3.7 nm, which could significantly facilitate the cooperative ON duplex hybridization. A pair of complementary 10-mer ON strands were used for protein conjugation. Each ON sequence had a pre-installed 5'-amine group, which was converted into a maleimide function using a commercially available hetero-functional linker. The protein-ON conjugation was accomplished via the maleimide-thiol chemistry. Two POC products were produced, each carrying four identical 10-mer ON strands. The ON domains of the two POC products were complementary. When annealing the two POCs in an equimolar ratio, 1D wire-like protein assemblies were observed in native agarose gel electrophoresis, cryo-TEM, and negative staining TEM. Neighboring protein monomers were uniformly organized by a face-to-face, bivalent ON duplex interaction. Additionally, when compared to the unconjugated control, the ON duplex domain of the wire-like protein assemblies showed an increased thermodynamic stability and a more rapid dissociation process in melting experiments. These results indicated that cooperative hybridization existed between the two closely positioned ON duplexes on the same protein surface. The presented work may inspire the directed assembly of various functional protein arrays programmed by specific valency of DNA duplex formations.

Despite the multimeric nature, all the above proteins were readily folded in bacterial expression before the ON conjugation. The directed assembly of ON-protein hybrid materials was mainly programmed via the base-pairing interactions between the conjugated-ON strands. The protein domains, however, contributed little to such self-assembly processes. It would be highly desirable to synchronize the protein-protein interaction with the ON-ON interaction in a controlled manner to create well-defined hybrid supramolecular assemblies. Tezcan and co-workers took the first step to orchestrate three different non-covalent interactions, including protein-protein interaction, ON duplex hybridization, and ON-protein interaction, to realize the self-assembly of nucleoprotein-like architectures (Figure 11C).⁶¹ A cytochrome *cb*₅₆₂ variant (RIDC3) was chosen as the protein domain. The protein-protein interaction was coordinated by Zn^{2+} , which could cause the protein to self-organize into 1D, 2D, and 3D arrays.¹⁰⁴ A cysteine residue was engineered into the protein surface for ON conjugation. A 10-mer ON duplex was chosen to connect two neighboring proteins. Such ON design matched the protein dimension, and the ON duplex binding strength was compatible with the Zn^{2+} -mediated protein-protein interaction. Each ON strand was designed to have a 5'-amine group, which was reacted with a hetero-functional linker to furnish the maleimide function. The protein-ON conjugation was carried out via Michael addition to provide two wanted POC building blocks. By mixing these two products in an equimolar ratio, the authors screened temperature, pH, POC concentrations, and Zn^{2+} equivalents. The ordered hybrid

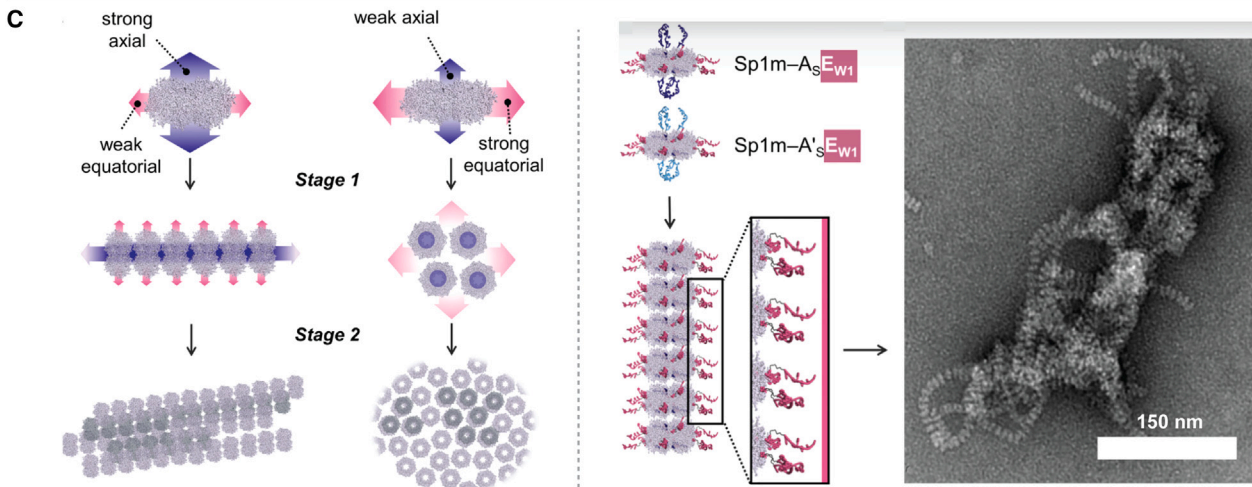
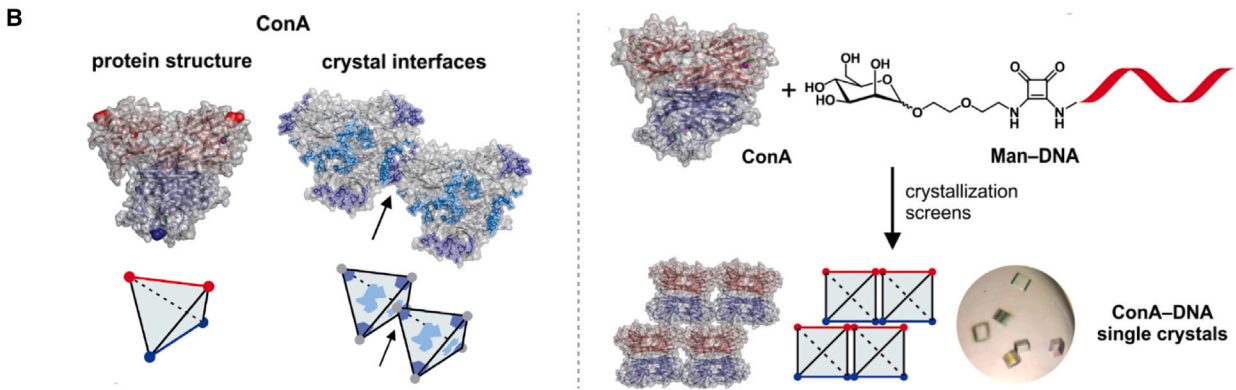
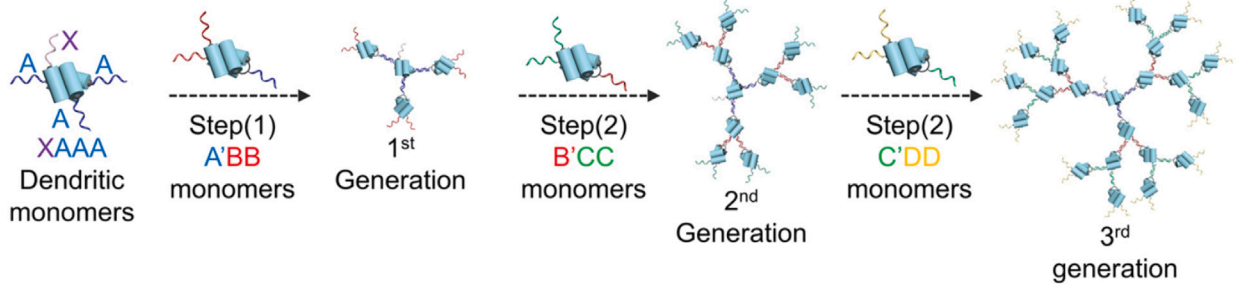
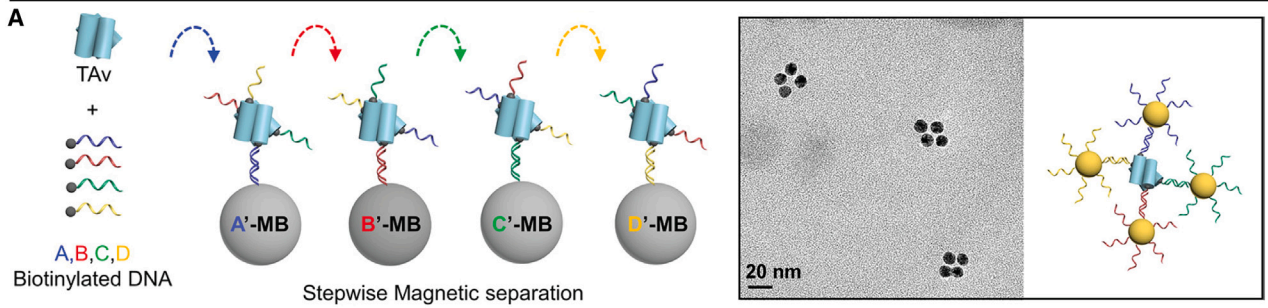


Figure 12. Protein-ON conjugates for various nanotechnological applications

(A) A user-friendly method to passivate the model protein with up to four different ON strands, which were further employed to compose trivalent hybrid synthon for programmed dendrimer assembly. Adapted with permission from Kim et al.⁶⁵ Copyright 2019, American Chemical Society.

(B) DNA duplex hybridization was used to reprogram the protein-protein interface contact in the crystal unit cells. Adapted with permission from Partridge et al.⁶⁸ Copyright 2021, American Chemical Society.

(C) Multiple hierarchical assembly of protein building blocks were engineered in a predefined manner via DNA duplex hybridization. Reproduced with permission from Hayes et al.⁵² Copyright 2021, National Academy of Sciences.

assemblies could form when all the following criteria were satisfied: (1) pH value between 4.75 and 5, (2) temperature from 4°C to 10°C, and (3) the molar ratio of Zn²⁺ and total POCs = 2–10. Beyond the given conditions, only small-size clustered aggregates (<100 nm) were produced. When the Zn²⁺ was missing, no ordered hybrid assemblies could be formed. This was further supported by the addition of ethylenediaminetetraacetic acid (Zn²⁺ chelator) into the preformed hybrid crystals, which were dissolved immediately. These results indicated that the Zn²⁺-coordinated protein-protein interaction played a pivotal role in promoting the hybrid crystal formation. In addition to such protein-protein contact, the ON duplex hybridization also contributed equally to the self-assembly of ordered aggregates. This was demonstrated by the following experiments. The preformed hybrid arrays quickly disappeared when the suspension was incubated higher than 40°C, at which the ON duplex dissociated. In the presence of Zn²⁺, the unmodified protein needed 1 week to grow into mature crystals. However, mixing two POC products could produce mature crystals within 4 h. The authors combined multiple techniques, including AFM, SEM, TEM, cryo-EM, SAXS, and computational simulation, to illustrate the putative cell unit of the hybrid crystals and the probable interactions within/between the cell units. One structural model was finally identified that fulfilled all chemical and crystallographic requirements. Based on this model, the authors reasoned that hydrogen bonds and salt bridges at the protein-ON duplex interface also contributed to stabilizing the putative architecture of hybrid materials. A delicate balance must be maintained between the protein domain and the ON domain to achieve structural cooperativity. For instance, slightly elongating the ON duplex from 10-mer to 12-mer could be accommodated; however, further extending it to 15-mer or shortening the original 10-mer to 8-mer already tilted the balance. This research opened immense possibilities for the bottom-up construction of various structurally tunable materials.

Modifying a single protein with multiple different ON sequences would bestow an extra layer of valency control on the hybrid nanoscale building blocks, thus opening a new chemical dimension for nanotechnological applications. However, synthesis of such a multivalent product is a tedious task. This usually demands that (1) the protein is properly engineered and (2) several orthogonal methods are rationally designed for *in situ* or sequential ON conjugations. Gratifyingly, Song and his team reported a simple method to passivate the model protein with up to four different ON strands in a user-friendly manner (Figure 12A).⁶⁵ The tetrameric protein traptavidin was chosen as the model protein. As a mutant variant of streptavidin, traptavidin showed an improved stability compared to the wild-type streptavidin upon binding to biotin. Four different 20-mer ON strands were designed to have a biotin function at the 5' end. By mixing the traptavidin and four biotinylated DNA strands in a 1:3 M ratio, a pool of POCs was produced. The corresponding ON complements were individually attached to four magnetic beads for sequential separation. The POC pool was then subjected to four stepwise separations using the ON complement-functionalized magnetic beads. Thus, the desirable POCs were successfully isolated in a decent overall yield (8.1%), where each binding site of tetrameric traptavidin was occupied by a different ON strand. The cascaded FRET analysis revealed that

the isolated products were composed of six constitutional isomers due to the inherently distinct tetravalency of ON-traptavidin conjugation. The tetravalent POCs were used to program the self-assembly of six different asymmetric plasmonic nanostructures. The same strategy was extended to compose hybrid synthons for programmed dendrimer assembly. For each synthon, two different ON strands were used for traptavidin conjugation, one having two biotin functions and the other having one biotin function. The former ON was first mixed with traptavidin to produce the monovalent intermediate upon magnetic bead separation. The resulting intermediate was then functionalized with two equivalents of the latter ON to afford the trivalent hybrid synthon. The obtained synthon was homogeneous due to the inherent mirror symmetry. Three different synthons were composed, with the conjugated-ON pattern as A'BB, B'CC, and C'DD. Seeded by the initial dendritic monomer (with three A strands), the author demonstrated the layer-by-layer assembly of up to third-generation dendrimer POC systems in a user-friendly manner. Both agarose gel electrophoresis and DLS measurement indicated that the dendrimer's average size gradually increased when moving from zeroth generation to third generation. This new methodology may open a new dimension toward the rational design of various hybrid nanoarchitectures with higher structural complexity for smart material and molecular theragnosis applications.

The DNA duplex hybridization strategy was also explored to reprogram the protein-protein interface contacts within the crystal unit cells to manipulate the morphology of protein crystals at a microscopic scale. In a recent study, using concanavalin A (ConA) as the model protein, Mirkin et al. demonstrated how to employ DNA duplex interactions to eliminate, enhance, or replace native protein-protein interactions to edit the protein packing within single crystals (Figure 12B).⁶⁸ ConA is a homotetrameric lectin and can selectively bind to mannose with a high affinity. There are four carbohydrate-binding sites on a single ConA, located at the four vertices of the tetrahedron-like protein surface. In the absence of mannose, one ConA can readily bind to another ConA via vertex-triangle plane interface contacts.¹⁰⁵ Surface amino acids around the mannose-binding site are engaged in the latter protein-protein interactions. The single crystals formed by ConA itself, as well as ConA-mannose complexes, have been well characterized. To introduce the DNA duplex interaction, a 4-mer self-complementary ON (5'-ATAT, having an amine group at the 5' end) was conjugated to an amino-modified mannose using the squaramide chemistry developed in the same paper. The desirable mannose-ON conjugate was obtained. When mixing the ConA and mannose-ON conjugate for crystallization, the morphology of single crystals was clearly changed relative to the ConA itself. The native proteins yielded crystals with a cubic morphology in the space group I222. However, the addition of the mannose-ON conjugate produced crystals with a thin plate morphology in the space group P2₁22₁. Interface analysis revealed that the original vertex-triangle plane protein-protein contact in the ConA crystals was reprogrammed to a new vertex-vertex ON duplex interaction along the b-direction and two sets of emergent protein-protein interactions in the a-c plane. Similar results were obtained using another three 4-mer self-complementary ONs as well as a pair of 4-mer complementary ONs. As expected, no single crystals could be obtained when the ON complementarity was lacking. When the ON sequence was elongated from 4-mer to 6-mer, the distance between two neighboring proteins was accordingly increased along the b-direction by ~7 Å. Moving the mannose conjugation from the 5' end to the middle of the 4-mer ON sequence could also significantly modulate the protein packing in single crystals. Overall, this work showcased an elegant example of using programmable DNA interactions to override natural protein-protein interactions to control the assembly of native proteins in a tailored manner. It is tantalizing to

anticipate that the proposed strategy can be advanced to realize precise control over various protein assembly pathways for the design and synthesis of novel functional biomaterials.

As a next step, relying on the DNA duplex hybridization strategy and the addressable anisotropic protein surface, Mirkin and co-workers successfully programmed multistep hierarchical assembly of protein building blocks in a predefined manner. In this study, stable protein 1 (Sp1) was chosen as the model system (Figure 12C).⁵² Sp1 is a symmetric homododecameric protein but is folded into an anisotropic hexagonal-prism shape. The protein surface was sorted into two disparate regions for ON conjugation, the top and bottom hexagonal faces in axial direction and all six rectangular side faces in equatorial direction. The axial and equatorial directions were designed to accommodate two different types of ONs, respectively. Therefore, an Sp1 variant was expressed to harbor solvent-accessible 24 primary amines at the axial direction (half on the top face, half on the bottom face) and 12 thiols at the equatorial direction. The Sp1 variant was first treated with a hetero-bifunctional linker (maleimide-azide) to convert the thiol functions to the azido functions at the equatorial direction. The resulting intermediate was then reacted with another hetero-bifunctional linker (NHS ester-tetrazine) to transform the primary amine groups to the tetrazine groups at the axial direction. Thus, the Sp1 variant was modified with two different click handles: tetrazines at the axial direction and azides at the equatorial direction. In parallel, two different types of ONs were designed to have two click partners, dibenzocyclooctyne (DBCO) and *trans*-cyclooctene (TCO), respectively. The Sp1-ON conjugations were accomplished in a one-pot reaction via two orthogonal click chemistries (azide/DBCO and tetrazine/cyclooctene). The two different types of ONs could form a strong dsDNA and a weak dsDNA. When only the ONs for strong dsDNA formation were introduced at the axial direction of the proteins, 1D protein chains were observed. In contrast, while the same ONs were furnished at the equatorial direction of the proteins, 2D arrays were produced. To explore the multistage assembly, the weak dsDNA contact was added into the above single-pathway systems. The resulting proteins were functionalized with two different types of ONs, one to make the strong dsDNA contacts and the other to do the weak dsDNA contacts. As in the single-pathway systems, the strong dsDNA contacts could drive the first-stage protein assembly to form 1D protein chains or 2D arrays, whereby the secondary ONs, which were conjugated to proteins to make the weak dsDNA contacts, were displayed in a multivalent fashion. This gave rise to an emergent interaction with strong cooperativity to drive the second-stage protein assembly to form higher-order nanostructures. Such two-step hierarchical assembly processes were confirmed by an FRET-based thermal denaturation assay. Other factors could also be used to fine-tune hierarchical assembly pathways, such as varying ion strength and integrating a third ON design as presented in the study. The multistep hierarchical assembly strategy encoded by the programmable DNA interactions holds promise to be extended to any protein or other nanoscale building blocks for composing novel biomaterials with improved structural complexity.

Proteins conjugated to DNA nanostructures as structural components

The simple 1D DNA domains, which were conjugated to proteins in the above examples, could be substituted by complicated 2D and 3D DNA nanostructures to further increase the structural programmability. This new strategy imposed a highly demanding task: the individual contributions from the two disparate self-assembling macromolecular domains must be orchestrated to maintain a delicate balance in the best way to be cooperative. Stephanopoulos et al. demonstrated an

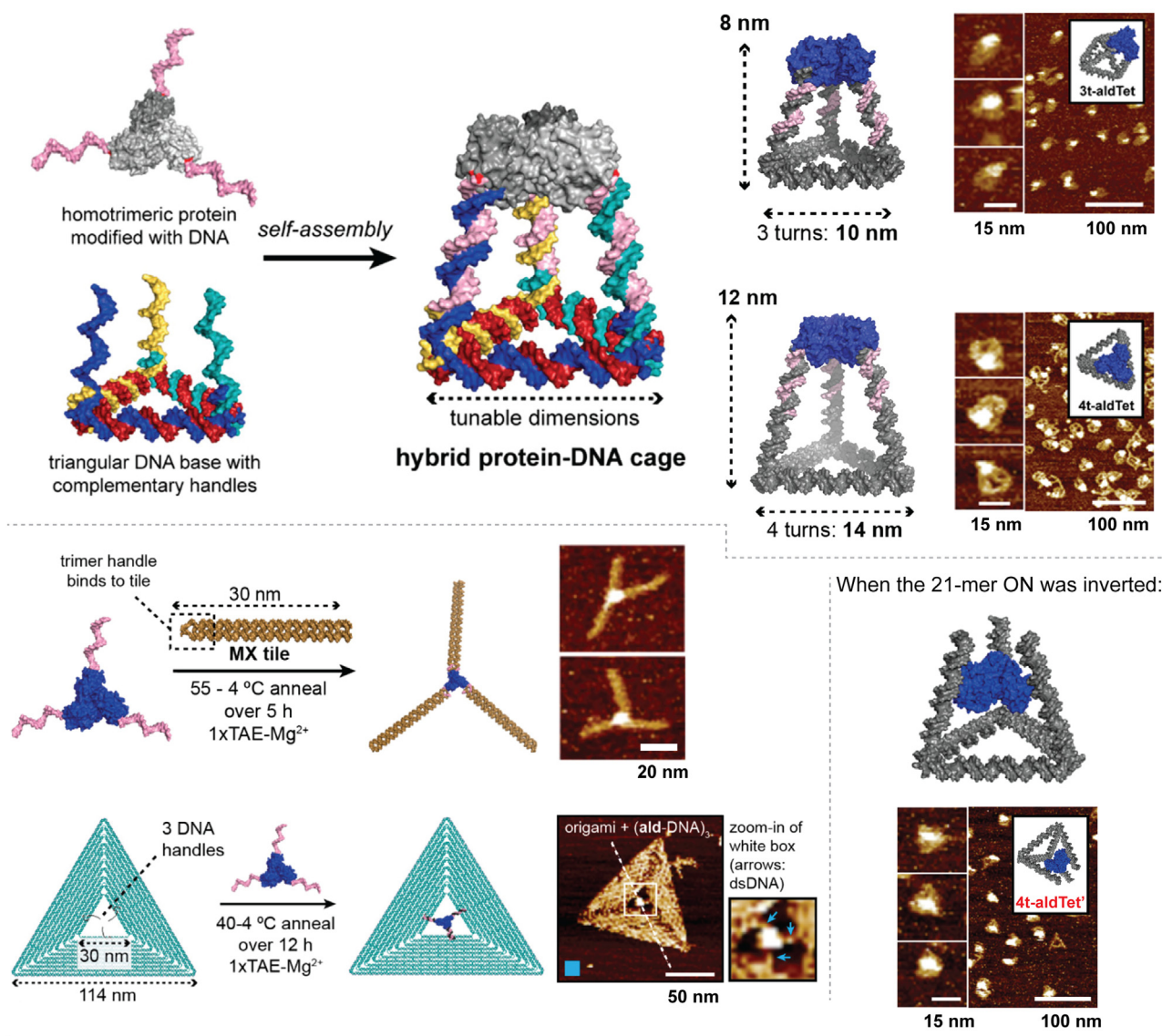


Figure 13. Bottom-up constructions of 2D hybrid three-arm multicrossover tiles, 2D hybrid triangle origami, and 3D hybrid tetrahedral cages
Adapted with permission from Xu et al.^{53,54} Copyright 2019, 2020, American Chemical Society.

excellent example of how to unite protein building blocks and 3D DNA nanostructures to program a series of 2D and 3D hybrid nanoarchitectures (Figure 13).^{53,54} In this work, 2-dehydro-3-deoxyphosphogluconate-aldolase (Ald) was chosen as the model protein. Ald is a homotrimeric protein and its surface is amenable to mutagenesis.¹⁰⁶ Moreover, this enzyme can tolerate relatively high temperatures, making it compatible with the DNA nanostructure annealing process. The inherent C_3 symmetry of Ald was used to engineer single-amino-acid mutations for ON conjugation. An Ald variant was designed by mutating a solvent-accessible glutamic acid residue to a cysteine in each monomeric subunit. As a result, the protein mutant had three peripheral surface positions available for covalently anchoring ONs. A 21-mer ON strand (having a 5'-amine group) was first treated with a hetero-bifunctional cross-linker to furnish the activated disulfide function. The resulting ON was conjugated to the Ald mutant via a thiol-exchange reaction. The

obtained POC product had three identical ON arms. Two different model DNA nanostructures were employed to validate the POC's trivalent property. A DNA multicrossover tile was extended to have the 21-mer ON complement. When mixed with the POC, native gel electrophoresis and AFM indicated that three multicrossover tiles could be attached to the core Ald protein via the trivalent ON duplex hybridization. The results were confirmed using a triangular DNA origami structure designed to immobilize one POC molecule in the central cavity via the same trivalent contacts.

The authors explored further how to use the POC product to self-assemble a series of hybrid tetrahedral nanocages. A third DNA nanostructure was designed to have a triangular base (every side was a 31-mer dsDNA) from which each vertex was extended to a DNA tether composed of a 10-bp dsDNA and the 21-mer ON complement. When mixed with the POC product, a hybrid tetrahedral nanocage was successfully assembled with all six edges possessing three helical turns. To demonstrate the structural programmability, a fourth DNA nanostructure was introduced. It had a similar morphology to the third one, but, when hybridizing to the POC, all six edges of the resulting nanocage were elongated to have four helical turns. As expected, a larger nanocage formation was observed in native gel electrophoresis and AFM analysis. The authors accidentally inverted the sequence direction of the 21-mer ON complement in their original study. Serendipitously, a tetrahedron-like shape was assembled via the same trivalent ON contacts.⁵⁴ Due to the spontaneous disulfide formation between the cysteine residues, an undesirable aggregation phenomenon was noticed for the Ald mutant. To circumvent this issue, the authors mutated the same solvent-accessible glutamic acid residue to an unnatural 4-azidophenylalanine to produce a second Ald mutant for ON conjugation. The same 21-mer ON strand (having a 5'-amine group) was treated with another hetero-bifunctional cross-linker to have the DBCO function. The Ald-ON conjugation was accomplished via the SPAAC reaction. When the obtained POC product was mixed with the third DNA nanostructure, highly similar nanocage morphology was observed with all six edges having three helical turns. The protein surface addressability was further demonstrated by moving the three ON conjugation sites from the outer edge to the same surface, positioning them closer to each other. In accord, a third POC product was synthesized. However, when mixing it with the third DNA nanostructure, open nanocages predominated where only monovalent ON duplex hybridization took place and the other two were fully dissociated. This unexpected result was ascribed to the possible intramolecular steric or electrostatic repulsion. This study may inspire merging self-assembling protein and DNA building blocks into a single macromolecule for the bottom-up construction of innovative nanomaterials, whereby the bioactivity of proteins and the programmability of DNA can be combined coherently to develop advanced nanotechnological tools.

CONCLUSIONS AND PERSPECTIVES

The integration of self-assembly principles in DNA and peptides/proteins allows an emerging paradigm for advanced chemical and nanotechnological applications. The main research rationale is to unite the high programmability of DNA and the versatile chemical functions of peptides/proteins into a new type of building-block-like nanoscale bricks where DNA and peptides/proteins can complement each other while circumventing their own imperfections. As highlighted in this tutorial review, significant progress has been made within the last decade to orchestrate DNA and peptides/proteins for cooperative assembly. Until now, most research has

been dedicated to making DNA and peptides/proteins work together in an effort to achieve favorable structural/functional synergy in the hybrid nanostructures. Those lead works laid the first steppingstones to demonstrate that the marriage between DNA and peptides/proteins was a successful strategy for nanotechnological applications, as well as showcasing its tremendous power for bottom-up construction of various nanoarchitectures that otherwise are impossible to achieve when using DNA or peptides/proteins alone.

Several challenges remain on the way, which may hamper the rapid development of hybrid DNA-peptide/protein nanostructures in the coming years. (1) Currently, no computational program (such as caDNAno¹⁰⁷ and TALOS¹⁰⁸ for DNA origami design and Rosetta¹⁰⁹ for peptide/protein structure design) is available to accommodate both DNA and peptides/proteins to assist the design and assembly of wanted hybrid nanostructures. At present, most studies are empirical and based on trial and error. The adaptation of a reliable computational program that can predict the self-assembly pathways of hybrid nanostructures will greatly promote the hybrid DNA-peptide/protein technology. (2) The number of conjugation methods is still limited, which severely hampers the sequential ligation between DNA and peptides or the site-specific modification of DNA to the anisotropic protein surfaces. Orthogonal chemistry has been widely exploited to covalently conjugate different peptides/proteins to DNA.^{35–55} However, cognate reaction handles need to be carefully introduced into both peptides/proteins and DNA, leading to tedious lab work and time-consuming purification processes. One possible direction is to hijack the well-established enzyme-mediated ligation methods (e.g., sortase A, butelase-1, peptidyl asparaginyl ligases, subtiligase) in protein chemistry¹¹⁰ to accomplish efficient DNA-peptide/protein crosslinking. In this case, natural peptides/proteins can be used, although recognition motifs still need to be specifically incorporated into DNA. In addition, non-covalent conjugation can be used with covalent methods to expand the structural diversity of the hybrid nanostructures. Finally, new chemistry development may further empower the arsenal of covalent and non-covalent DNA-peptide/protein conjugation methods. (3) Almost all hybrid DNA-peptide/protein nanostructures in the literature are in their thermodynamically stable states. However, recapitulating the kinetic and transient molecular states is extremely important for many biological processes. For example, the rational design of a dissipative system composed of DNA and peptides/proteins would become a milestone for hybrid nanodevice and nanorobot development. (4) Peptides/proteins have been explored intensively to understand their structure-function relationships. However, we have limited knowledge of how they interact with DNA. The polyanionic nature of DNA may influence the folding topologies and the chemical functions of peptides/proteins when placed in proximity. Likewise, the peptides/proteins could reciprocally influence the structural integrity of DNA domains. This can be resolved when more structural studies of hybrid nanostructures are reported.

Similar hybrid nanoscale architectures also exist in nature; for instance, nucleoproteins and protein-nucleic acid complexes play pivotal roles in biological processes such as ribosomes, RNA-peptide complexes, viruses, and transient peptide-nucleic acid droplet formations. Looking to the horizon, a greater vision is to imitate nature to synergize DNA and peptides/proteins for the bottom-up construction of exquisite nanoscale machines and artificial organelles that are comparable to the natural counterparts or even surpass their biological functionalities. Beyond DNA and peptides/proteins, other biomolecules, such as RNA, saccharides, and lipids, can also be incorporated into hybrid nanostructures when properly designed. This may

ultimately pave an avenue toward the *de novo* design of artificial life forms such as viruses, bacteria, and cells in the future.

ACKNOWLEDGMENTS

H.M. and C.L. are grateful for financial support from the Lundbeck Foundation, Denmark, grant number R346-2020-1890. C.L. acknowledges the Villum Foundation, Denmark, for funding the Biomolecular Nanoscale Engineering Center (BioNEC), a VILLUM center of excellence, grant number VKR18333.

AUTHOR CONTRIBUTIONS

H.M. and C.L. proposed the topic of the review. M.B.D. and C.L. wrote the first draft. M.B.D. and C.L. produced the figures. M.B.D., H.M., and C.L. contributed to finalizing the manuscript.

DECLARATION OF INTERESTS

The authors declare no competing interests.

REFERENCES

- Seeman, N.C. (1982). Nucleic acid junctions and lattices. *J. Theor. Biol.* 99, 237–247. [https://doi.org/10.1016/0022-5193\(82\)90002-9](https://doi.org/10.1016/0022-5193(82)90002-9).
- Seeman, N.C. (2003). DNA in a material world. *Nature* 421, 427–431. <https://doi.org/10.1038/nature01406>.
- Rothmund, P.W.K. (2006). Folding DNA to create nanoscale shapes and patterns. *Nature* 440, 297–302. <https://doi.org/10.1038/nature04586>.
- Zhu, Y., Wu, J., and Zhou, Q. (2023). Functional DNA sensors integrated with nucleic acid signal amplification strategies for non-nucleic acid targets detection. *Biosens. Bioelectron.* 230, 115282. <https://doi.org/10.1016/j.bios.2023.115282>.
- Zhou, J., and Rossi, J. (2017). Aptamers as targeted therapeutics: current potential and challenges. *Nat. Rev. Drug Discov.* 16, 181–202. <https://doi.org/10.1038/nrd.2016.199>.
- Yang, L.F., Ling, M., Kacherovsky, N., and Pun, S.H. (2023). Aptamers 101: aptamer discovery and in vitro applications in biosensors and separations. *Chem. Sci.* 14, 4961–4978. <https://doi.org/10.1039/D3SC00439B>.
- McConnell, E.M., Cozma, I., Mou, Q., Brennan, J.D., Lu, Y., and Li, Y. (2021). Biosensing with DNAAzymes. *Chem. Soc. Rev.* 50, 8954–8994. <https://doi.org/10.1039/D1CS00240F>.
- He, L., Huang, R., Xiao, P., Liu, Y., Jin, L., Liu, H., Li, S., Deng, Y., Chen, Z., Li, Z., and He, N. (2021). Current signal amplification strategies in aptamer-based electrochemical biosensor: A review. *Chin. Chem. Lett.* 32, 1593–1602. <https://doi.org/10.1016/j.ccl.2020.12.054>.
- Kulkarni, J.A., Witzigmann, D., Thomson, S.B., Chen, S., Leavitt, B.R., Cullis, P.R., and van der Meel, R. (2021). The current landscape of nucleic acid therapeutics. *Nat. Nanotechnol.* 16, 630–643. <https://doi.org/10.1038/s41565-021-00898-0>.
- Rinaldi, C., and Wood, M.J.A. (2018). Antisense oligonucleotides: the next frontier for treatment of neurological disorders. *Nat. Rev. Neurol.* 14, 9–21. <https://doi.org/10.1038/nrneuro.2017.148>.
- Dalla Pozza, M., Abdullrahman, A., Cardin, C.J., Gasser, G., and Hall, J.P. (2022). Three's a crowd – stabilisation, structure, and applications of DNA triplexes. *Chem. Sci.* 13, 10193–10215. <https://doi.org/10.1039/D2SC01793H>.
- Bidar, N., Amini, M., Oroojalian, F., Baradaran, B., Hosseini, S.S., Shahbazi, M.-A., Hashemzaei, M., Mokhtarzadeh, A., Hamblin, M.R., and de la Guardia, M. (2021). Molecular beacon strategies for sensing purpose. *Trends Anal. Chem.* 134, 116143. <https://doi.org/10.1016/j.trac.2020.116143>.
- Qin, S., Tang, X., Chen, Y., Chen, K., Fan, N., Xiao, W., Zheng, Q., Li, G., Teng, Y., Wu, M., and Song, X. (2022). mRNA-based therapeutics: powerful and versatile tools to combat diseases. *Signal Transduct. Targeted Ther.* 7, 166. <https://doi.org/10.1038/s41392-022-01007-w>.
- Simmel, F.C., Yurke, B., and Singh, H.R. (2019). Principles and applications of nucleic acid strand displacement reactions. *Chem. Rev.* 119, 6326–6369. <https://doi.org/10.1021/acs.chemrev.8b00580>.
- Seeman, N.C., and Sleiman, H.F. (2017). DNA nanotechnology. *Nat. Rev. Mater.* 3, 17068. <https://doi.org/10.1038/natrevmats.2017.68>.
- Crooke, S.T., Witztum, J.L., Bennett, C.F., and Baker, B.F. (2018). RNA-targeted therapeutics. *Cell Metabol.* 27, 714–739. <https://doi.org/10.1016/j.cmet.2018.03.004>.
- Paunovska, K., Loughrey, D., and Dahlman, J.E. (2022). Drug delivery systems for RNA therapeutics. *Nat. Rev. Genet.* 23, 265–280. <https://doi.org/10.1038/s41576-021-00439-4>.
- Zhan, P., Peil, A., Jiang, Q., Wang, D., Mousavi, S., Xiong, Q., Shen, Q., Shang, Y., Ding, B., Lin, C., et al. (2023). Recent advances in DNA origami-engineered nanomaterials and applications. *Chem. Rev.* 123, 3976–4050. <https://doi.org/10.1021/acs.chemrev.3c00028>.
- Huang, P.-S., Boyken, S.E., and Baker, D. (2016). The coming of age of *de novo* protein design. *Nature* 537, 320–327. <https://doi.org/10.1038/nature19946>.
- Adler-Abramovich, L., and Gazit, E. (2014). The physical properties of supramolecular peptide assemblies: from building block association to technological applications. *Chem. Soc. Rev.* 43, 6881–6893. <https://doi.org/10.1039/C4CS00164H>.
- Pinter, T.B.J., Koebeke, K.J., and Pecoraro, V.L. (2020). Catalysis and electron transfer in *de novo* designed helical scaffolds. *Angew. Chem. Int. Ed.* 59, 7678–7699. <https://doi.org/10.1002/anie.201907502>.
- Pan, X., and Kortemme, T. (2021). Recent advances in *de novo* protein design: principles, methods, and applications. *J. Biol. Chem.* 296, 100558. <https://doi.org/10.1016/j.jbc.2021.100558>.
- Chalkley, M.J., Mann, S.I., and DeGrado, W.F. (2022). *De novo* metalloprotein design. *Nat. Rev. Chem.* 6, 31–50. <https://doi.org/10.1038/s41570-021-00339-5>.
- Stephanopoulos, N. (2020). Hybrid nanostructures from the self-assembly of proteins and DNA. *Chem* 6, 364–405. <https://doi.org/10.1016/j.chempr.2020.01.012>.
- Higashi, S.L., Rozi, N., Hanifah, S.A., and Ikeda, M. (2020). Supramolecular architectures of nucleic acid/peptide hybrids. *Int. J. Mol. Sci.* 21, 9458. <https://doi.org/10.3390/ijms21249458>.
- Zhao, D., Kong, Y., Zhao, S., and Xing, H. (2020). Engineering functional DNA–protein conjugates for biosensing, biomedical, and nanoassembly applications. *Top. Curr. Chem.* 378, 41. <https://doi.org/10.1007/s41061-020-00305-7>.

27. MacCulloch, T., Buchberger, A., and Stephanopoulos, N. (2019). Emerging applications of peptide–oligonucleotide conjugates: bioactive scaffolds, self-assembling systems, and hybrid nanomaterials. *Org. Biomol. Chem.* 17, 1668–1682. <https://doi.org/10.1039/C8OB02436G>.
28. Daly, M.L., Klawa, S.J., and Freeman, R. (2020). New functions emerging from peptide–DNA materials. In *Peptide-based Biomaterials*, M.O. Guler, ed. (The Royal Society of Chemistry), pp. 459–486. <https://doi.org/10.1039/9781839161148-00459>.
29. dos Remedios, C.G., Chhabra, D., Kekic, M., Dedova, I.V., Tsubakihara, M., Berry, D.A., and Nosworthy, N.J. (2003). Actin binding proteins: regulation of cytoskeletal microfilaments. *Physiol. Rev.* 83, 433–473. <https://doi.org/10.1152/physrev.00026.2002>.
30. Abraham, J.N., Gour, N., Bolisetty, S., Mezzenga, R., and Nardin, C. (2015). Controlled aggregation of peptide–DNA hybrids into amyloid-like fibrils. *Eur. Polym. J.* 65, 268–275. <https://doi.org/10.1016/j.eurpolymj.2015.02.009>.
31. Gour, N., Abraham, J.N., Chami, M., Castillo, A., Verma, S., and Vebert-Nardin, C. (2014). Label-free, optical sensing of the supramolecular assembly into fibrils of a ditryptophan–DNA hybrid. *Chem. Commun.* 50, 6863–6865. <https://doi.org/10.1039/C4CC02631D>.
32. Gour, N., Kedracki, D., Safir, I., Ngo, K.X., and Vebert-Nardin, C. (2012). Self-assembling DNA–peptide hybrids: morphological consequences of oligonucleotide grafting to a pathogenic amyloid fibrils forming dipeptide. *Chem. Commun.* 48, 5440–5442. <https://doi.org/10.1039/C2CC31458D>.
33. Strable, E., Johnson, J.E., and Finn, M.G. (2004). Natural nanochemical building blocks: icosahedral virus particles organized by attached oligonucleotides. *Nano Lett.* 4, 1385–1389. <https://doi.org/10.1021/nl0493850>.
34. Hafenstine, G.R., Domaille, D.W., Cha, J.N., and Goodwin, A.P. (2015). Self-assembly and reassembly of fiber-forming dipeptides for pH-triggered DNA delivery. *J. Polym. Sci., Part A: Polym. Chem.* 53, 183–187. <https://doi.org/10.1002/pola.27319>.
35. Chotera, A., Sadihov, H., Cohen-Luria, R., Monnard, P.-A., and Ashkenasy, G. (2018). Functional assemblies emerging in complex mixtures of peptides and nucleic acid–peptide chimeras. *Chem. Eur. J.* 24, 10128–10135. <https://doi.org/10.1002/chem.201800500>.
36. Ghosh, P.S., and Hamilton, A.D. (2012). Noncovalent template-assisted mimicry of multiloop protein surfaces: assembling discontinuous and functional domains. *J. Am. Chem. Soc.* 134, 13208–13211. <https://doi.org/10.1021/ja305360q>.
37. Goetzfried, M.A., Voge, K., Mückl, A., Kaiser, M., Holland, N.B., Simmel, F.C., and Pirzer, T. (2019). Periodic Operation of a dynamic DNA origami structure utilizing the hydrophilic–hydrophobic phase-transition of stimulus-sensitive polypeptides. *Small* 15, 1903541. <https://doi.org/10.1002/sml.201903541>.
38. Kye, M., and Lim, Y.b. (2016). Reciprocal self-assembly of peptide–DNA conjugates into a programmable sub-10-nm supramolecular deoxyribonucleoprotein. *Angew. Chem. Int. Ed.* 55, 12003–12007. <https://doi.org/10.1002/anie.201605696>.
39. Wang, B., Pan, R., Zhu, W., Xu, Y., Tian, Y., Endo, M., Sugiyama, H., Yang, Y., and Qian, X. (2021). Short intrinsically disordered polypeptide–oligonucleotide conjugates for programmed self-assembly of nanospheres with temperature-dependent size controllability. *Soft Matter* 17, 1184–1188. <https://doi.org/10.1039/D0SM01817A>.
40. Yao, S., Liao, Y., Pan, R., Zhu, W., Xu, Y., Yang, Y., and Qian, X. (2022). Programmed co-assembly of DNA–peptide hybrid microdroplets by phase separation. *Chin. Chem. Lett.* 33, 1545–1549. <https://doi.org/10.1016/j.ccl.2021.08.116>.
41. Cigler, P., Lytton-Jean, A.K.R., Anderson, D.G., Finn, M.G., and Park, S.Y. (2010). DNA-controlled assembly of a NaI lattice structure from gold nanoparticles and protein nanoparticles. *Nat. Mater.* 9, 918–922. <https://doi.org/10.1038/nmat2877>.
42. Kye, M., Zhang, Z., and Lim, Y.-b. (2021). Self-assembling cyclic peptide–oligonucleotide conjugates: synthetic strategies and the effect of cyclic topology on self-assembly and base pairing. *Pept. Sci.* 113, e24193. <https://doi.org/10.1002/pep.2.24193>.
43. Lou, C., Martos-Maldonado, M.C., Madsen, C.S., Thomsen, R.P., Midtgaard, S.R., Christensen, N.J., Kjems, J., Thulstrup, P.W., Wengel, J., and Jensen, K.J. (2016). Peptide–oligonucleotide conjugates as nanoscale building blocks for assembly of an artificial three-helix protein mimic. *Nat. Commun.* 7, 12294. <https://doi.org/10.1038/ncomms12294>.
44. Lou, C., Christensen, N.J., Martos-Maldonado, M.C., Midtgaard, S.R., Ejlersen, M., Thulstrup, P.W., Sørensen, K.K., Jensen, K.J., and Wengel, J. (2017). Folding topology of a short coiled-coil peptide structure templated by an oligonucleotide triplex. *Chem. Eur. J.* 23, 9297–9305. <https://doi.org/10.1002/chem.201700971>.
45. Freeman, R., Han, M., Álvarez, Z., Lewis, J.A., Wester, J.R., Stephanopoulos, N., McClendon, M.T., Lynsky, C., Godbe, J.M., Sangji, H., et al. (2018). Reversible self-assembly of superstructured networks. *Science* 362, 808–813. <https://doi.org/10.1126/science.aat6141>.
46. Lou, C., Boesen, J.T., Christensen, N.J., Sørensen, K.K., Thulstrup, P.W., Pedersen, M.N., Giralt, E., Jensen, K.J., and Wengel, J. (2020). Self-assembly of DNA–peptide supermolecules: coiled-coil peptide structures templated by D-DNA and L-DNA triplexes exhibit chirality-independent but orientation-dependent stabilizing cooperativity. *Chem. Eur. J.* 26, 5676–5684. <https://doi.org/10.1002/chem.201905636>.
47. Daly, M.L., Gao, Y., and Freeman, R. (2019). Encoding reversible hierarchical structures with supramolecular peptide–DNA materials. *Bioconjugate Chem.* 30, 1864–1869. <https://doi.org/10.1021/acs.bioconjchem.9b00271>.
48. Pandey, S., Mandal, S., Danielsen, M.B., Brown, A., Hu, C., Christensen, N.J., Kulakova, A.V., Song, S., Brown, T., Jensen, K.J., et al. (2022). Chirality transmission in macromolecular domains. *Nat. Commun.* 13, 76. <https://doi.org/10.1038/s41467-021-27708-4>.
49. Buchberger, A., Simmons, C.R., Fahmi, N.E., Freeman, R., and Stephanopoulos, N. (2020). Hierarchical assembly of nucleic acid/coiled-coil peptide nanostructures. *J. Am. Chem. Soc.* 142, 1406–1416. <https://doi.org/10.1021/jacs.9b11158>.
50. Brodin, J.D., Auyeung, E., and Mirkin, C.A. (2015). DNA-mediated engineering of multicomponent enzyme crystals. *Proc. Natl. Acad. Sci. USA* 112, 4564–4569. <https://doi.org/10.1073/pnas.1503533112>.
51. McMillan, J.R., Brodin, J.D., Millan, J.A., Lee, B., Olvera de la Cruz, M., and Mirkin, C.A. (2017). Modulating nanoparticle superlattice structure using proteins with tunable bond distributions. *J. Am. Chem. Soc.* 139, 1754–1757. <https://doi.org/10.1021/jacs.6b11893>.
52. Hayes, O.G., Partridge, B.E., and Mirkin, C.A. (2021). Encoding hierarchical assembly pathways of proteins with DNA. *Proc. Natl. Acad. Sci. USA* 118, e2106808118. <https://doi.org/10.1073/pnas.2106808118>.
53. Xu, Y., Jiang, S., Simmons, C.R., Narayanan, R.P., Zhang, F., Aziz, A.-M., Yan, H., and Stephanopoulos, N. (2019). Tunable nanoscale cages from self-assembling DNA and protein building blocks. *ACS Nano* 13, 3545–3554. <https://doi.org/10.1021/acsnano.8b09798>.
54. Xu, Y., Jiang, S., Simmons, C.R., Narayanan, R.P., Zhang, F., Aziz, A.-M., Yan, H., and Stephanopoulos, N. (2020). Correction to tunable nanoscale cages from self-assembling DNA and protein building blocks. *ACS Nano* 14, 7673. <https://doi.org/10.1021/acsnano.0c02484>.
55. Jin, J., Baker, E.G., Wood, C.W., Bath, J., Woolfson, D.N., and Turberfield, A.J. (2019). Peptide assembly directed and quantified using megadalton DNA nanostructures. *ACS Nano* 13, 9927–9935. <https://doi.org/10.1021/acsnano.9b04251>.
56. Marchán, V., Ortega, S., Pulido, D., Pedrosa, E., and Grandas, A. (2006). Diels–Alder cycloadditions in water for the straightforward preparation of peptide–oligonucleotide conjugates. *Nucleic Acids Res.* 34, e24. <https://doi.org/10.1093/nar/gnj020>.
57. Borsenberger, V., and Howorka, S. (2009). Diene-modified nucleotides for the Diels–Alder-mediated functional tagging of DNA. *Nucleic Acids Res.* 37, 1477–1485. <https://doi.org/10.1093/nar/gkn1066>.
58. Oliveira, B.L., Guo, Z., and Bernardes, G.J.L. (2017). Inverse electron demand Diels–Alder reactions in chemical biology. *Chem. Soc. Rev.* 46, 4895–4950. <https://doi.org/10.1039/C7CS00184C>.
59. Kashiwagi, D., Sim, S., Niwa, T., Taguchi, H., and Aida, T. (2018). Protein nanotube selectively cleavable with DNA:

- supramolecular polymerization of "DNA-appended molecular chaperones". *J. Am. Chem. Soc.* **140**, 26–29. <https://doi.org/10.1021/jacs.7b09892>.
60. McMillan, J.R., and Mirkin, C.A. (2018). DNA-functionalized, bivalent proteins. *J. Am. Chem. Soc.* **140**, 6776–6779. <https://doi.org/10.1021/jacs.8b03403>.
 61. Subramanian, R.H., Smith, S.J., Alberstein, R.G., Bailey, J.B., Zhang, L., Cardone, G., Suominen, L., Chami, M., Stahlberg, H., Baker, T.S., and Tezcan, F.A. (2018). Self-assembly of a designed nucleoprotein architecture through multimodal interactions. *ACS Cent. Sci.* **4**, 1578–1586. <https://doi.org/10.1021/acscentsci.8b00745>.
 62. Spruijt, E., Tusk, S.E., and Bayley, H. (2018). DNA scaffolds support stable and uniform peptide nanopores. *Nat. Nanotechnol.* **13**, 739–745. <https://doi.org/10.1038/s41565-018-0139-6>.
 63. Nakamura, Y., Yamada, S., Nishikawa, S., and Matsuura, K. (2017). DNA-modified artificial viral capsids self-assembled from DNA-conjugated β -annulus peptide. *J. Pept. Sci.* **23**, 636–643. <https://doi.org/10.1002/psc.2967>.
 64. Stephanopoulos, N., Freeman, R., North, H.A., Sur, S., Jeong, S.J., Tantakitti, F., Kessler, J.A., and Stupp, S.I. (2015). Bioactive DNA-peptide nanotubes enhance the differentiation of neural stem cells into neurons. *Nano Lett.* **15**, 603–609. <https://doi.org/10.1021/nl504079q>.
 65. Kim, Y.-Y., Bang, Y., Lee, A.-H., and Song, Y.-K. (2019). Multivalent traptavidin–DNA conjugates for the programmable assembly of nanostructures. *ACS Nano* **13**, 1183–1194. <https://doi.org/10.1021/acsnano.8b06170>.
 66. Zhang, C., Tian, C., Guo, F., Liu, Z., Jiang, W., and Mao, C. (2012). DNA-directed three-dimensional protein organization. *Angew. Chem. Int. Ed.* **51**, 3382–3385. <https://doi.org/10.1002/anie.201108710>.
 67. Howarth, M., Chinnapen, D.J.F., Gerrow, K., Dorrestein, P.C., Grandy, M.R., Kelleher, N.L., El-Husseini, A., and Ting, A.Y. (2006). A monovalent streptavidin with a single femtomolar biotin binding site. *Nat. Methods* **3**, 267–273. <https://doi.org/10.1038/nmeth861>.
 68. Partridge, B.E., Winegar, P.H., Han, Z., and Mirkin, C.A. (2021). Redefining protein interfaces within protein single crystals with DNA. *J. Am. Chem. Soc.* **143**, 8925–8934. <https://doi.org/10.1021/jacs.1c04191>.
 69. Goodman, R.P., Erben, C.M., Malo, J., Ho, W.M., McKee, M.L., Kapanidis, A.N., and Turberfield, A.J. (2009). A facile method for reversibly linking a recombinant protein to DNA. *Chembiochem* **10**, 1551–1557. <https://doi.org/10.1002/cbic.200900165>.
 70. Shen, W., Zhong, H., Neff, D., and Norton, M.L. (2009). NTA directed protein nanopatterning on DNA origami nanoconstructs. *J. Am. Chem. Soc.* **131**, 6660–6661. <https://doi.org/10.1021/ja901407j>.
 71. Rosen, C.B., Kodal, A.L.B., Nielsen, J.S., Schaffert, D.H., Scavanius, C., Okholm, A.H., Voigt, N.V., Enghild, J.J., Kjems, J., Tørring, T., and Gothelf, K.V. (2014). Template-directed covalent conjugation of DNA to native antibodies, transferrin and other metal-binding proteins. *Nat. Chem.* **6**, 804–809. <https://doi.org/10.1038/nchem.2003>.
 72. Ni, R., and Chau, Y. (2014). Structural Mimics of Viruses Through Peptide/DNA Co-Assembly. *J. Am. Chem. Soc.* **136**, 17902–17905. <https://doi.org/10.1021/ja507833x>.
 73. Liu, Y., Lin, C., Li, H., and Yan, H. (2005). Aptamer-directed self-assembly of protein arrays on a DNA nanostructure. *Angew. Chem. Int. Ed.* **44**, 4333–4338. <https://doi.org/10.1002/anie.200501089>.
 74. Rosier, B.J.H.M., Cremers, G.A.O., Engelen, W., Merckx, M., Brunsveld, L., and de Greef, T.F.A. (2017). Incorporation of native antibodies and Fc-fusion proteins on DNA nanostructures via a modular conjugation strategy. *Chem. Commun.* **53**, 7393–7396. <https://doi.org/10.1039/C7CC04178K>.
 75. Nakata, E., Liew, F.F., Uwatoko, C., Kiyonaka, S., Mori, Y., Katsuda, Y., Endo, M., Sugiyama, H., and Morii, T. (2012). Zinc-finger proteins for site-specific protein positioning on DNA-origami structures. *Angew. Chem. Int. Ed.* **51**, 2421–2424. <https://doi.org/10.1002/anie.201108199>.
 76. Ngo, T.A., Nakata, E., Saimura, M., and Morii, T. (2016). Spatially organized enzymes drive cofactor-coupled cascade reactions. *J. Am. Chem. Soc.* **138**, 3012–3021. <https://doi.org/10.1021/jacs.5b10198>.
 77. Kurokawa, T., Kiyonaka, S., Nakata, E., Endo, M., Koyama, S., Mori, E., Tran, N.H., Dinh, H., Suzuki, Y., Hidaka, K., et al. (2018). DNA origami scaffolds as templates for functional tetrameric Kir3 K⁺ channels. *Angew. Chem. Int. Ed.* **57**, 2586–2591. <https://doi.org/10.1002/anie.201709982>.
 78. Nguyen, T.M., Nakata, E., Saimura, M., Dinh, H., and Morii, T. (2017). Design of modular protein tags for orthogonal covalent bond formation at specific DNA sequences. *J. Am. Chem. Soc.* **139**, 8487–8496. <https://doi.org/10.1021/jacs.7b01640>.
 79. Reches, M., and Gazit, E. (2003). Casting metal nanowires within discrete self-assembled peptide nanotubes. *Science* **300**, 625–627. <https://doi.org/10.1126/science.1082387>.
 80. Colletier, J.-P., Laganowsky, A., Landau, M., Zhao, M., Soriaga, A.B., Goldschmidt, L., Flot, D., Cascio, D., Sawaya, M.R., and Eisenberg, D. (2011). Molecular basis for amyloid- β polymorphism. *Proc. Natl. Acad. Sci. USA* **108**, 16938–16943. <https://doi.org/10.1073/pnas.1112600108>.
 81. Walshaw, J., and Woolfson, D.N. (2001). SOCKET: a program for identifying and analysing coiled-coil motifs within protein structures. *J. Mol. Biol.* **307**, 1427–1450. <https://doi.org/10.1006/jmbi.2001.4545>.
 82. Ogihara, N.L., Weiss, M.S., Degrado, W.F., and Eisenberg, D. (1997). The crystal structure of the designed trimeric coiled coil coil-VaLd: implications for engineering crystals and supramolecular assemblies. *Protein Sci.* **6**, 80–88. <https://doi.org/10.1002/pro.5560060109>.
 83. Krautwald, S., and Carreira, E.M. (2017). Stereodivergence in asymmetric catalysis. *J. Am. Chem. Soc.* **139**, 5627–5639. <https://doi.org/10.1021/jacs.6b13340>.
 84. Proctor, R.S.J., Colgan, A.C., and Phipps, R.J. (2020). Exploiting attractive non-covalent interactions for the enantioselective catalysis of reactions involving radical intermediates. *Nat. Chem.* **12**, 990–1004. <https://doi.org/10.1038/s41557-020-00561-6>.
 85. Neel, A.J., Hilton, M.J., Sigman, M.S., and Toste, F.D. (2017). Exploiting non-covalent π interactions for catalyst design. *Nature* **543**, 637–646. <https://doi.org/10.1038/nature21701>.
 86. Le Bailly, B.A.F., and Clayden, J. (2016). Dynamic foldamer chemistry. *Chem. Commun.* **52**, 4852–4863. <https://doi.org/10.1039/C6CC00788K>.
 87. Yashima, E., Ousaka, N., Taura, D., Shimomura, K., Ikai, T., and Maeda, K. (2016). Supramolecular helical systems: helical assemblies of small molecules, foldamers, and polymers with chiral amplification and their functions. *Chem. Rev.* **116**, 13752–13990. <https://doi.org/10.1021/acs.chemrev.6b00354>.
 88. Ha, S.C., Lowenhaupt, K., Rich, A., Kim, Y.-G., and Kim, K.K. (2005). Crystal structure of a junction between B-DNA and Z-DNA reveals two extruded bases. *Nature* **437**, 1183–1186. <https://doi.org/10.1038/nature04088>.
 89. Majd, S., Yusko, E.C., Billeh, Y.N., Macrae, M.X., Yang, J., and Mayer, M. (2010). Applications of biological pores in nanomedicine, sensing, and nanoelectronics. *Curr. Opin. Biotechnol.* **21**, 439–476. <https://doi.org/10.1016/j.copbio.2010.05.002>.
 90. Clarke, J., Wu, H.-C., Jayasinghe, L., Patel, A., Reid, S., and Bayley, H. (2009). Continuous base identification for single-molecule nanopore DNA sequencing. *Nat. Nanotechnol.* **4**, 265–270. <https://doi.org/10.1038/nnano.2009.12>.
 91. Ouldali, H., Sarthak, K., Ensslen, T., Piguot, F., Manivet, P., Pelta, J., Behrends, J.C., Aksimentiev, A., and Oukhaled, A. (2020). Electrical recognition of the twenty proteinogenic amino acids using an aerolysin nanopore. *Nat. Biotechnol.* **38**, 176–181. <https://doi.org/10.1038/s41587-019-0345-2>.
 92. Jain, M., Koren, S., Miga, K.H., Quick, J., Rand, A.C., Sasani, T.A., Tyson, J.R., Beggs, A.D., Dilthey, A.T., Fiddes, I.T., et al. (2018). Nanopore sequencing and assembly of a human genome with ultra-long reads. *Nat. Biotechnol.* **36**, 338–345. <https://doi.org/10.1038/nbt.4060>.
 93. Van der Verren, S.E., Van Gerven, N., Jonckheere, W., Hambley, R., Singh, P., Kilgour, J., Jordan, M., Wallace, E.J., Jayasinghe, L., and Remaut, H. (2020). A dual-constriction biological nanopore resolves homonucleotide sequences with high fidelity. *Nat. Biotechnol.* **38**, 1415–1420. <https://doi.org/10.1038/s41587-020-0570-8>.
 94. Howorka, S. (2017). Building membrane nanopores. *Nat. Nanotechnol.* **12**, 619–630. <https://doi.org/10.1038/nnano.2017.99>.

95. Huang, G., Voet, A., and Maglia, G. (2019). FraC nanopores with adjustable diameter identify the mass of opposite-charge peptides with 44 dalton resolution. *Nat. Commun.* *10*, 835. <https://doi.org/10.1038/s41467-019-08761-6>.
96. Mahendran, K.R., Niitsu, A., Kong, L., Thomson, A.R., Sessions, R.B., Woolfson, D.N., and Bayley, H. (2017). A monodisperse transmembrane α -helical peptide barrel. *Nat. Chem.* *9*, 411–419. <https://doi.org/10.1038/nchem.2647>.
97. Rotem, D., Jayasinghe, L., Salichou, M., and Bayley, H. (2012). Protein detection by nanopores equipped with aptamers. *J. Am. Chem. Soc.* *134*, 2781–2787. <https://doi.org/10.1021/ja2105653>.
98. Gilbert, R.J.C., Bayley, H., and Anderluh, G. (2017). Membrane pores: from structure and assembly, to medicine and technology. *Philos. Trans. R. Soc. Lond. B Biol. Sci.* *372*, 20160208. <https://doi.org/10.1098/rstb.2016.0208>.
99. Buchberger, A., Riker, K., Bernal-Chanchavac, J., Narayanan, R.P., Simmons, C.R., Fahmi, N.E., Freeman, R., and Stephanopoulos, N. (2022). Bioactive fibronectin-III10–DNA origami nanofibers promote cell adhesion and spreading. *ACS Appl. Bio Mater.* *5*, 4625–4634. <https://doi.org/10.1021/acsbm.2c00303>.
100. Urry, D.W. (1997). Physical chemistry of biological free energy transduction as demonstrated by elastic protein-based polymers. *J. Phys. Chem. B* *101*, 11007–11028. <https://doi.org/10.1021/jp972167t>.
101. He, Y., Ye, T., Su, M., Zhang, C., Ribbe, A.E., Jiang, W., and Mao, C. (2008). Hierarchical self-assembly of DNA into symmetric supramolecular polyhedra. *Nature* *452*, 198–201. <https://doi.org/10.1038/nature06597>.
102. Zhang, C., Su, M., He, Y., Zhao, X., Fang, P.-a., Ribbe, A.E., Jiang, W., and Mao, C. (2008). Conformational flexibility facilitates self-assembly of complex DNA nanostructures. *Proc. Natl. Acad. Sci. USA* *105*, 10665–10669. <https://doi.org/10.1073/pnas.0803841105>.
103. He, Y., Su, M., Fang, P.-a., Zhang, C., Ribbe, A.E., Jiang, W., and Mao, C. (2010). On the chirality of self-assembled DNA octahedra. *Angew. Chem. Int. Ed.* *49*, 748–751. <https://doi.org/10.1002/anie.200904513>.
104. Brodin, J.D., Ambroggio, X.I., Tang, C., Parent, K.N., Baker, T.S., and Tezcan, F.A. (2012). Metal-directed, chemically tunable assembly of one-two- and three-dimensional crystalline protein arrays. *Nat. Chem.* *4*, 375–382. <https://doi.org/10.1038/nchem.1290>.
105. Parkin, S., Rupp, B., and Hope, H. (1996). Atomic resolution structure of concanavalin A at 120 K. *Acta Crystallogr. D: Struct. Biol.* *52*, 1161–1168. <https://doi.org/10.1107/S0907444996009237>.
106. Patterson, D.P., Desai, A.M., Holl, M.M.B., and Marsh, E.N.G. (2011). Evaluation of a symmetry-based strategy for assembling protein complexes. *RSC Adv.* *1*, 1004–1012. <https://doi.org/10.1039/C1RA00282A>.
107. Douglas, S.M., Marblestone, A.H., Teerapittayanon, S., Vazquez, A., Church, G.M., and Shih, W.M. (2009). Rapid prototyping of 3D DNA-origami shapes with caDNAno. *Nucleic Acids Res.* *37*, 5001–5006. <https://doi.org/10.1093/nar/gkp436>.
108. Jun, H., Shepherd, T.R., Zhang, K., Bricker, W.P., Li, S., Chiu, W., and Bathe, M. (2019). Automated sequence design of 3D polyhedral wireframe DNA origami with honeycomb edges. *ACS Nano* *13*, 2083–2093. <https://doi.org/10.1021/acsnano.8b08671>.
109. Leman, J.K., Weitzner, B.D., Lewis, S.M., Adolf-Bryfogle, J., Alam, N., Alford, R.F., Aprahamian, M., Baker, D., Barlow, K.A., Barth, P., et al. (2020). Macromolecular modeling and design in Rosetta: recent methods and frameworks. *Nat. Methods* *17*, 665–680. <https://doi.org/10.1038/s41592-020-0848-2>.
110. Morgan, H.E., Turnbull, W.B., and Webb, M.E. (2022). Challenges in the use of sortase and other peptide ligases for site-specific protein modification. *Chem. Soc. Rev.* *51*, 4121–4145. <https://doi.org/10.1039/DOCS01148G>.